ORNL Resolved Resonance Covariance Generation for ENDF/B-VII.1

L. Leal*, K. Guber, D. Wiarda, G. Arbanas, H. Derrien, R. Sayer, N. Larson,M. Dunn
Oak Ridge National Laboratory, P.O. Box 2008, Oak Ridge, TN 37831-6354, USA
(Received 8 August 2011; revised 23 September 2011; 2nd revised 27 August 2012; accepted 27 September 2012)

Resonance-parameter covariance matrix (RPCM) evaluations in the resolved resonance region were done at the Oak Ridge National Laboratory (ORNL) for the chromium isotopes, titanium isotopes, ^{19}F, ^{58}Ni, ^{60}Ni, ^{35}Cl, ^{37}Cl, ^{39}K, ^{41}K, ^{55}Mn, ^{233}U, ^{235}U, ^{238}U, and ^{239}Pu using the computer code SAMMY. The retroactive approach of the code SAMMY was used to generate the RPCMs for ^{233}U. For ^{235}U, the approach used for covariance generation was similar to the retroactive approach with the distinction that real experimental data were used as opposed to data generated from the resonance parameters. RPCMs for ^{238}U and ^{239}Pu were generated together with the resonance parameter evaluations. The RPCMs were then converted in the ENDF format using the FILE32 representation. Alternatively, for computer storage reasons, the FILE32 was converted in the FILE33 cross section covariance matrix (CSCM). Both representations were processed using the computer code PUFF-IV. This paper describes the procedures used to generate the RPCM and CSCM in the resonance region for ENDF/B-VII.1. The impact of data uncertainty in nuclear reactor benchmark calculations is also presented.

Contents

I. INTRODUCTION 3501

II. METHODOLOGY 3502
A. Brief Description of the SAMMY Code for Resonance Covariance Evaluation 3502
B. AMPX/PUFF-IV: Description of Cross Section and Covariance Processing 3504

III. Covariance Evaluation 3504
A. Chromium Isotopes Evaluation 3504
B. Titanium Isotopes Evaluation 3504
C. Fluorine ^{19}F Evaluation 3506
D. Nickel ^{58}Ni and ^{60}Ni Evaluation and Covariance 3507
E. Chlorine ^{35}Cl and ^{37}Cl Resonance Evaluations Including Covariance 3508
F. Potassium ^{39}K and ^{41}K Evaluations Including Covariance 3510
G. Manganese ^{55}Mn Resonance Evaluation 3511

IV. Covariance Evaluation for Major Actinides 3513
A. Covariance Evaluations for ^{233}U 3513
B. Covariance Evaluations for ^{235}U 3513
C. Covariance Evaluations for ^{238}U 3514
D. Covariance Evaluations for ^{239}Pu 3514
E. Benchmark Calculations and Data Uncertainty 3515

V. Summary and Conclusions 3516

Acknowledgments 3517

References 3517

I. INTRODUCTION

Design targets for nuclear systems have demanded better basic nuclear data and greater knowledge of their uncertainties. Hence, over the years efforts have been made to improve the quality of basic nuclear data. Thermal reactor designs and fissionable applications, such as criticality safety, have been the driving force for new data evaluations in the low-energy range. Data evaluations in the high-energy region have been accomplished primarily in support of shielding applications and fast reactor design. Although the accuracy of the nuclear data (such as neutron interaction cross sections) has significantly improved, until recently, little information existed on nuclear data uncertainties, and even less existed on nuclear data covariances. At Oak Ridge National Laboratory (ORNL), data evaluations in the resolved and unresolved resonance energy regions are performed with the computer code SAMMY [1]. Using SAMMY, uncertainties are incorporated in the evaluation of the experimental data (transmission or total cross section, capture, and fission cross section). Various sources of experimental uncertainties must be included; among these are

*Corresponding author, electronic address: leallc@ornl.gov

normalization, background, neutron time-of-flight, sample thickness, and temperature. All of these uncertainties are included in the evaluation process in order to properly determine the RPCMs. In this paper, we address the generation of covariance data in the resonance region via the computer code SAMMY. Two approaches are used in SAMMY for the generation of resonance-parameter covariance data: During the evaluation process, SAMMY generates a set of resonance parameters that fit the data; in addition, SAMMY provides the resonance-parameter covariance. For existing resonance parameter evaluations, where no resonance-parameter covariance data are available, the alternative is to use an approach called retroactive resonance-parameter covariance generation; this approach is described in some detail in this paper. This paper provides documentation on the covariance evaluations in the resolved resonance region that have been performed for ENDF/B-VII.1. Details on the data measurements and cross section evaluations are given in Ref. [2].

II. METHODOLOGY

First, we will elaborate on some of the ENDF nomenclature used in this article. In the ENDF format the distinction among the resonance formalism is made by using the flag named LRF. As an example, LRF=3 indicates that the formalism used in the resonance evaluation is in the Reich-Moore formalism. Specifically, LRF=7 indicates the use of the Reich-Moore formalism with the inclusion of channels (inelastic for instance) other than the usual scattering, capture and fission channels. This representation is also called in ENDF the "R-Matrix Limited". There exist several options to represent covariance data in FILE32 of the ENDF library that are indicated by the use of the flag denominated LCOMP. For LCOMP=1 the variance and covariance for resonance parameters are given explicitly. However, if there exist a large number of resonance parameters the LCOMP=1 may not be appropriate due to computer storage limitations. For this the LCOMP=2 option allows the data to be presented in a compact format.

The resonance analysis of the experimental data performed with SAMMY uses the R-matrix formalism for treating the resonances and the Bayes' theorem for the fitting process. In a sequential Bayes analysis, the RPCM obtained from the analysis of one data set is used in the analysis of the next data set. If the experimental data sets were thoroughly consistent, this procedure should yield a unique set of resonance parameters with a corresponding RPCM. However, in practice this is usually not possible, since the experimental data carry systematic uncertainties due to the normalization process, background correction, neutron energy calibration, and others. Because of these systematic uncertainties, an experimental database obtained by retrieving all the available data is rarely consistent and the evaluator has to choose which data is included in the evaluation. A short explanation of the procedure for evaluating the experimental data and the generation of the RPCM will be given for several resonance evaluations performed at ORNL that are part of the ENDF/B-VII.1 (VII.1) nuclear data library.

There are two evaluations presented in the following, namely ^{35}Cl and ^{19}F, that use the LRF=7 option for representing resonance parameters. The LRF=7 format was introduced to address limitations of the LRF=3 format, since its representation of resonance parameters in ENDF corresponds to the Reich-Moore formalism with only two particle outgoing channels. Although the LRF=7 is a more elaborate format allowing many entrance and outgoing channels it is still limited. One of the limitations, for instance, is the non-hard-sphere phase shift feature which is not included in the format. The covariance representation in the resonance region for the majority of resonance evaluations included in VII.1 are done with the LCOMP=1 option. However, the representation for ^{35}Cl is based on the LCOMP=2, that is, the compact formalism for covariance. The LCOMP=2 format was developed to alleviate computer storage by dropping small correlations and rounding large values and storing the results as integers.

A. Brief Description of the SAMMY Code for Resonance Covariance Evaluation

The computer code SAMMY has been developed and maintained at ORNL for use in the evaluation of experimental data in the resolved and unresolved resonance energy regions. In SAMMY a RPCM can be generated in two ways: a) as a result of the evaluation process in which SAMMY generates a set of resonance parameters that fits the data together with the corresponding RPCM; b) by generating the RPCM from a pre-existing set of resonance parameters using the retroactive approach when RPCM is no longer available. In the evaluations performed nowadays, covariance information is preserved and included in the nuclear data files. Here a brief description of the retroactive approach for generating RPCM is given. Resonance parameters for many nuclides are available in ENDF FILE2, but when it is not possible to completely redo the analysis of the experimental data, the following scheme may be used to generate a realistic approximation for the covariance matrix.

- Retrieve "best set" of available resonance parameters from the data libraries.
- Use the parameters to generate cross sections for total, scattering, fission, and capture cross sections for input to SAMMY.
- Realistic experimental conditions (Doppler/Debye temperature, resolution function, *etc.*) are assumed.

- Assign "experimental" uncertainties to the generated data based on the uncertainty in the thermal capture cross section and the capture resonance integral, data normalization, data background, *etc.* Also, the experimental uncertainties when available in the EXFOR data base were used, as well as information from the literature.
- Run the SAMMY code with the option to generate resonance covariances retroactively.
- Convert the resonance covariance results from SAMMY into the ENDF FILE32 format. The resulting resonance parameters and covariances are used in the calculations of average cross sections and uncertainties. Even though the diagonal element seems to be arbitrary, there is some relation to experiments since information from literature and data banks is used.

The generated data are then analyzed simultaneously using generalized least-squares equations as the fitting procedure. The values for the covariance matrix V_{ij} are derived from the statistical uncertainties on the individual data points and from the uncertainties on the data-reduction parameters. This can be written in the usual fashion

$$V_{ij} = v_i\delta_{ij} + \sum_k [g_{ik}(\Delta r_k)^2 g_{jk}], \tag{1}$$

where v_i is the diagonal component that contains statistical errors due to the measurements, Δr_k represents the uncertainty on the kth data-reduction parameter r_k, and g_{ik} is the partial derivative of the cross section at energy E_i with respect to r_k .

With P_m being a member of a set of resonance parameters for which we wish to determine the covariance matrix, and T_i being the theoretical value of the described experimental quantity at energy E_i, we can write in matrix notation the least-squares equations as follows

$$\begin{aligned} P' &= P + M'G^tV^{-1}(D-T), \\ M' &= (G^tV^{-1}G)^{-1}. \end{aligned} \tag{2}$$

Here P' represents the updated set of resonance parameters and M' the associated RPCM, G is the set of partial derivatives of the theoretical values T with respect to the resonance parameters P. G is also referred to as the sensitivity matrix. Because we are analyzing artificially created data, P' is very nearly identical to P; this follows directly from Eq. 2 when $D = T$. However, if real physical quantities were analyzed, P' would be different from P. The matrix M', which was derived as the covariance matrix associated with the updated parameters, is therefore an appropriate representation for the resonance parameter covariance matrix associated with the original set of resonance parameters P. It should be noted that when real experimental data along with their uncertainties are used, the retroactive procedure described above is no longer used; instead, real covariances are derived from experimental data.

In the following we describe the methodology used in the evaluations reported here, unless otherwise stated (*e.g.* see section III.D). First, experimental data with as many details as possible are gathered, preferably new experimental data, with all the known issues associated with older experiments, such as incorrect weighting function, neutron sensitivity, *etc.*, having been avoided. When suitable existing experimental data from the EXFOR database is used together with thermal values, this data was inspected for suitability for inclusion in the experimental data base for the evaluation. At the start of a resonance evaluation, a prior set of resonance parameter was generated using literature and the resonance files from the nuclear data libraries. Usually this parameter set already contains an estimate of the scattering radius and some spin assignments. However, the procedure used to generate the spin of the resonance is based on the statistical analysis of the resonance parameters [3],[4]. In this approach the probability that a resonance having a certain value of $g\Gamma_n$ is an l-wave resonance provides insight into the resonance spin. In addition sometimes a trial-and-error approach is also used to determine which spin combination provides the best fit of the data. External resonances describe the potential scattering cross section effects for the energy region where the evaluation is performed. An inaccurate representation of the external contribution may lead to problems in the SAMMY evaluation procedure, causing difficulties in the production of a set of resonance parameters that fit all the experimental data in a consistent manner. The methodology used to determine the external levels consists of shifting the resonances in the region where the evaluation is made into external regions below and above the resonance evaluation region. In this approach the neutron widths are adjusted in such a way that the neutron strength function is preserved. The experimental data used in the evaluations presented in this paper, unless explicitly stated, were usually measured at room temperature. Also, for the calculation of the Doppler broadening of the cross section, the free gas model and corresponding Debye temperature was used. In the SAMMY fit of the experimental data, systematic uncertainties were propagated into the final RPCM, unless otherwise stated. Concerning the uncertainties for the ORELA data used in the new evaluations, we make the following general statements. The largest uncertainty in the ORELA capture data is usually the normalization, which ranges from 1.5 to 3%. The pulse-height weighting function is known to be better than 3% and other uncertainties, such as n-flux monitor, dead-time, sample, γ-ray attenuation in sample and gain-shift, are about 1.5%. The experiments were performed with the goal to achieve a statistical uncertainty of about 10% at 200 keV neutron energy for sample and background measurements. ORELA transmission experiments can achieve a signal-to-background ratio of up to 0.1%. The background corrections for ambi-

ent, overlap, and (n,γ) on hydrogen are small compared to counting statistics. Normalization problems are circumvented by cycling the samples every 10 minutes with post run consistency check on scalers.

For each resonance evaluation with the SAMMY code, a RPCM was generated, which was implemented in either FILE32 or FILE33 in the ENDF data bank. For the nickel isotopes, in addition to the RPCM, the cross section covariance evaluation was also done, as explained in section III.D. The RPCMs were converted in the ENDF format using the LCOMP=1 option and processed with PUFF-IV module of AMPX-6, unless otherwise stated. Also for illustration the RPCM was processed with the PUFF-IV using the SCALE 44-group neutron group structure. An issue to note in this context is the sometimes small uncertainty for a group cross-section. This can be explained from the fact that the sensitivity to a small cross section is small. Since the uncertainty in the cross section is calculated by multiplying the sensitivity (derivative of the cross section with respect to the resonance parameters) with the resonance parameter covariance, and hence the final cross section uncertainty for the group cross section may be small. It should also be noted that in practical applications the variances (diagonal terms) are used in conjunction to the covariance (off-diagonal terms). Therefore, a simple cursory interpretation of cross section uncertainty figures may not be enough to assure whether or not the uncertainty in the cross section is appropriate (*e.g.* see Fig. 18).

B. AMPX/PUFF-IV: Description of Cross Section and Covariance Processing

The AMPX code system [5] is a collection of computer programs used to process nuclear data in the ENDF format. AMPX is written in Fortran 90 and allows for a more modular design, thus facilitating future upgrades. The primary tasks consist of generating multigroup and continuous-energy cross sections for nuclear applications. In addition, the AMPX is a modular code system that can be used to perform a wide variety of cross section processing tasks. AMPX-6 can be used to generate multigroup cross section libraries in various formats for use with modern transport codes. Continuous-energy cross section libraries can also be produced for use in Monte Carlo codes and other applications. One feature of the AMPX code system is the capability to process cross section uncertainty information into multigroup covariance matrices that can subsequently be used in radiation transport sensitivity analyses. These analyses are performed with the PUFF module [6] of AMPX. The PUFF-IV code processes ENDF-formatted cross section covariance data into multigroup covariance matrices. PUFF-IV handles all resonance parameter covariance formats in the resolved resonance region. Some features of the PUFF-IV code are the following:

- Improved processing of the LRF=7 resonance parameter covariance;
- Support for Basic Linear Algebra Subprograms (BLAS) to decrease computation time in the resolved resonance range;
- Support for user-defined flux functions;
- Module to convert COVERX format into NJOY BOX format.

Presently, PUFF-IV cannot process covariance information for energy and angular distributions of secondary particles. PUFF-IV does not process covariance information in Files 34 and 35; nor does it process covariance information in FILE40. The processing of these formats will be addressed in a future version of PUFF.

III. COVARIANCE EVALUATION

A. Chromium Isotopes Evaluation

Resolved resonance parameter evaluations [7] for chromium isotopes, namely ^{50}Cr, ^{52}Cr, ^{53}Cr, and ^{54}Cr, were done with the computer code SAMMY. The descriptions of the measured data used in the evaluation are indicated in Table I. The determination of the resolved resonance parameters for the chromium isotope below 100 keV relied mainly on the recent ORELA measurements done by Guber *et al.* [8]. The ORELA capture cross section data were essential in the evaluation since there are no good-quality and high-resolution capture cross section data available in the databanks. In addition to the new ORELA measurements, existing high-resolution transmission data for enriched nuclides were also included in the evaluation [9]. Thermal cross section data available in the EXFOR data system were also included in the evaluation.

The resonance regions for each chromium isotope were extended by taking advantage of the new high-resolution ORELA capture data and existing transmission data. Comparisons of the energy range for the evaluation generated in this work with existing evaluations are show in Table II. To illustrate the use of the RPCM, the uncertainties in the total, capture, and scattering cross sections at the thermal energy for ^{52}Cr and ^{53}Cr are displayed in Table III. Also listed in Table III are the results of VII.0 and that of the Atlas of Neutron Resonance (ANR) [10]. Covariance for ^{52}Cr for the capture and elastic scattering cross sections are shown in Fig. 1 and Fig. 2, respectively.

B. Titanium Isotopes Evaluation

Titanium is an effective absorbent that serves as baseline material for separation in high-activity waste solutions. Titanium has not been considered for use in

TABLE I: Experimental ORELA transmission and capture data used for the Cr evaluation.

Data Set	Ref.	Energy Range (keV)	Flight Path (m)	Density (at/b)
Natural Chromium				
Transmission	[8]	0.01 - 600	79.827	0.0531
Transmission	[8]	0.01 - 600	79.827	0.0263
Capture	[8]	0.01 - 600	38.414	0.0263
^{50}Cr				
Transmission	[9]	90 - 800	201.575	0.0607
^{52}Cr				
Transmission	[9]	80 - 1450	201.575	0.0606
Transmission	[9]	80 - 1450	201.575	0.0395
^{53}Cr				
Transmission	[8]	0.01 - 600	79.827	0.0056
Transmission	[8]	0.01 - 600	79.827	0.0180
Capture	[8]	0.01 - 600	40.116	0.0137
Transmission	[9]	60 - 600	201.575	0.0593
^{54}Cr				
Transmission	[9]	13 - 850	201.575	0.0541

TABLE II: Range of energy for existing and new evaluations.

Isotope	Energy Range (OLD)		Energy Range (NEW)	
^{50}Cr	10^{-5} eV	600 keV	10^{-5} eV	783 keV
^{52}Cr	10^{-5} eV	1.2 MeV	10^{-5} eV	1.43 MeV
^{53}Cr	10^{-5} eV	245 keV	10^{-5} eV	564 keV
^{54}Cr	10^{-5} eV	750 keV	10^{-5} eV	834 keV

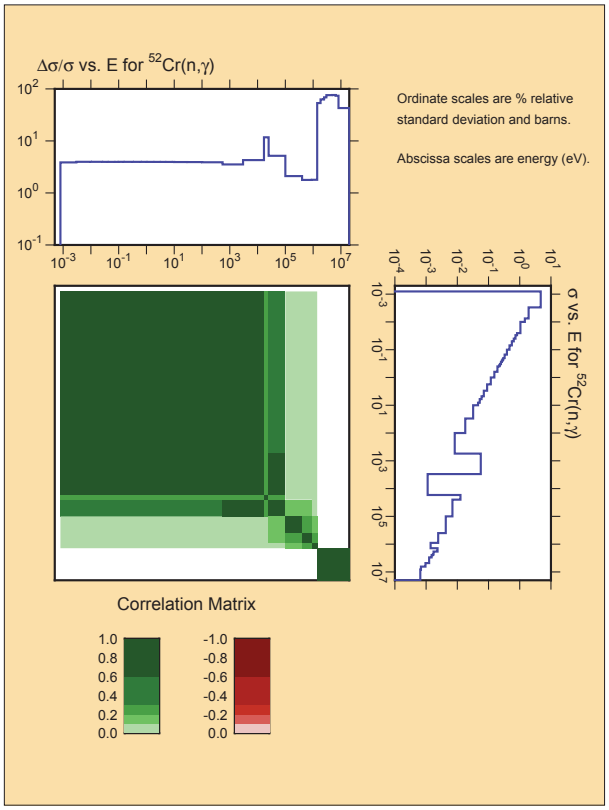

FIG. 1: Covariance for the ^{52}Cr capture cross section in the resolved resonance and high-energy regions.

nuclear applications such as reactor design and analysis. Rather, it normally appears as a structural material that may be present in fuel cycle facilities or canisters for transport and disposition of nuclear waste. Criticality safety evaluations of systems in which titanium is present require an understanding of the nuclear data and its uncertainty. To improve the cross section data and uncertainty for titanium in the thermal and epithermal energy regions a resolved resonance parameter and covariance evaluation for ^{48}Ti was done with the computer code SAMMY[11]. New capture and transmission measurements for enriched ^{48}Ti and natural titanium were made at the ORELA [12]. The neutron transmission and capture data were measured in the energy range from 10 eV to 500 keV. The transmission data were measured with a 80-meter flight-path length, whereas a 40-meter flight-path length was used for the capture cross section measurements. Since there are no previous capture cross-section measurements available in the resonance region, the ORELA data were vital for determining the shape and the uncertainty in the capture cross section. The descriptions of the measured data used in the evaluation are compiled in Table IV. The resonance evaluation for ^{48}Ti was done in the energy range from 10^{-5} eV to 400 keV. Thermal cross section data available in the EXFOR data system were also used in the evaluation. A RPCM was generated for ^{48}Ti as a result of the evaluation with the SAMMY. Since no quality data was available, no new resonance evaluation was done for ^{46}Ti, ^{47}Ti, ^{49}Ti, and ^{50}Ti, instead the retroactive approach was used to obtain the covariances for these isotopes. The uncertainties in the total, capture, and scattering cross sections at the thermal energy for ^{48}Ti are displayed in Table V. Also listed in Table V are the results reported in ANR. The capture resonance integral and uncertainty calculated with the RPCM is 3.78±0.17 barns; for the ANR the value is 3.90±0.25 barns, whereas for VII.0 the value is 3.68 barns. The covariance for ^{48}Ti for the capture cross section is shown in Fig. 3.

TABLE III: Chromium thermal cross sections and their uncertainties.

Isotope	Cross Section	VII.1	VII.0	ANR
^{52}Cr	Capture (b)	0.86 ± 0.02	0.75	0.86 ± 0.02
	Total (b)	3.93 ± 0.01	3.73	3.82 ± 0.03
	Scattering (b)	3.07 ± 0.07	2.99	2.96 ± 0.02
^{53}Cr	Capture (b)	18.41±0.51	18.06	18.60±0.6
	Total (b)	26.39±0.28	25.99	26.38±0.62
	Scattering (b)	7.98±0.28	7.92	7.78±0.2

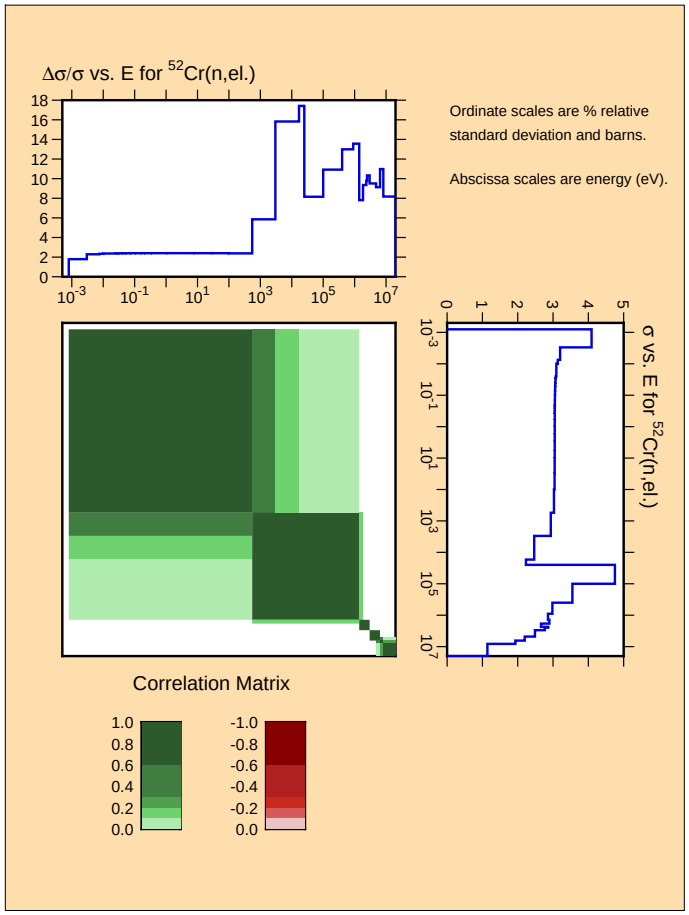

FIG. 2: Covariance for the ^{52}Cr scattering cross section in the resolved resonance and high-energy regions.

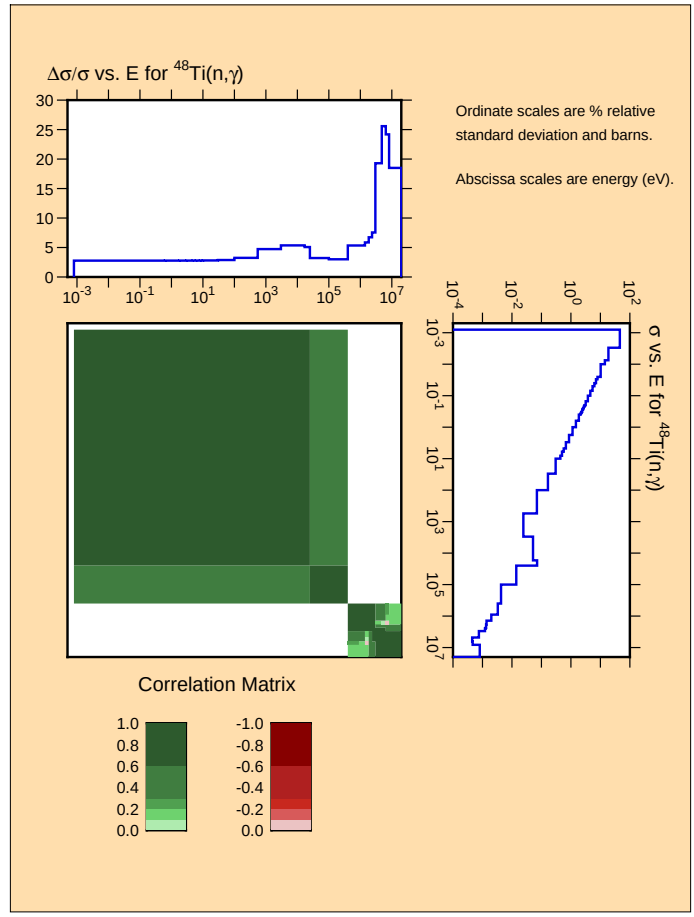

FIG. 3: Covariance for the ^{48}Ti capture cross section in resolved resonance and high-energy regions.

TABLE IV: Experimental ORELA transmission and capture data base for titanium.

Data Set	Ref.	Energy Range (keV)	Flight Path (m)	Density (at/b)
Natural Titanium				
Transmission	[12]	0.01 - 500	79.827	0.0530
Transmission	[12]	0.01 - 500	79.827	0.0088
Capture	[12]	0.01 - 500	40.116	0.0352
^{48}Ti (99.32 %)				
Transmission	[12]	0.01 - 500	79.827	0.0282
Transmission	[12]	0.01 - 500	79.827	0.0012
Capture	[12]	0.01 - 500	40.116	0.0091

TABLE V: Titanium thermal cross sections and their uncertainties.

Isotope	Cross Section	VII.1	VII.0	ANR
^{48}Ti	Capture (b)	8.32±0.23	7.84	8.32±0.16
	Total (b)	12.35±0.3	12.16	12.42±0.25
	Scattering (b)	4.03±0.17	4.32	4.10±0.2

C. Fluorine ^{19}F Evaluation

The resonance parameters for ^{19}F were obtained from a sequential SAMMY analysis of the experimental neutron transmission data, capture cross sections, and inelastic cross sections in the resolved energy region up to 1 MeV [13]. ^{19}F has two inelastic channels which are opening at the energies 109.9 keV with spin 1/2- and 197.2 keV with spin 5/2+, respectively. This evaluation is the first in the resolved resonance region that includes the inelastic cross section and makes use of the extended Reich-Moore formalism. The ENDF representation for the resonance parameter was done with the LRF=7 option. The set of experimental data used in the evaluation consisted of three transmission measurements of Larson [14] with thicknesses of 0.131 at/b, 0.0169 at/b, and 0.0242 at/b, respectively, measured on the 80-m flight path at the ORELA from 0.2 to 20 MeV. Also included was one capture cross section measurement by Guber [15] measured at ORELA up to 700 keV and three inelastic cross section measurements done by Broder [16] up to 1 MeV. In the neutron energy range up to 1 MeV, 2 *s*-wave, 5 *p*-wave, 17 *d*-wave, and 7 *f*-wave resonances were identified. The resonance parameters with the LRF=7 representa-

TABLE VI: Fluorine thermal cross sections and their uncertainties.

Isotope	Cross Section	VII.1	VII.0	ANR
^{19}F	Capture (mb)	9.50±0.1	9.58	9.51±0.09
	Total (b)	3.75±0.07	3.75	-
	Scattering (b)	3.74±0.07	3.74	3.64±0.01

tion were then processed with the POLIDENT module of the AMPX-6 system. It was found that the POLIDENT results were identical to those calculated with SAMMY. For the thermal cross section we have used the total cross section data of Rainwater[17] in the energy region from thermal to 5 eV. The Rainwater total cross section data were in agreement with the effective total cross section derived from the ORNL thick sample transmission data. No data normalization was needed for the Rainwater total cross section. At the time of the evaluation, the most recent capture cross section measurement of Raman *et al.* [18] at thermal energy was used. To fit the capture cross section data at low energy, the ENDF/B-VII ^{19}F capture cross section evaluation, normalized to the Raman thermal data, was used. Covariances for the resonance parameters was generated in the resolved energy region with SAMMY. The results for the thermal cross section calculated with the resonance parameters and uncertainties with the RPCM are shown in Table VI. Also displayed in Table VI are the results calculated with VII.0 together with the results quoted in the ANR. The covariance for the capture crosses section calculated with the PUFF-IV code is displayed in Fig. 4.

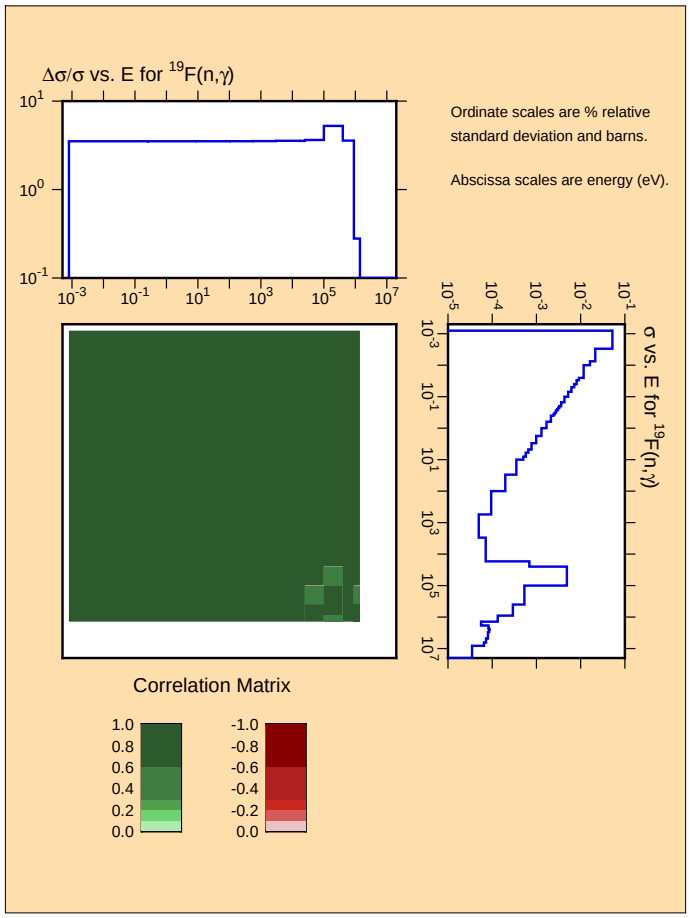

FIG. 4: Covariance for the ^{19}F capture cross section in resolved resonance region.

D. Nickel ^{58}Ni and ^{60}Ni Evaluation and Covariance

Resonance region evaluations of ^{58}Ni and ^{60}Ni [19] started with the VII.0 resonance parameters as prior values, in neutron energy ranges thermal to 812 keV for ^{58}Ni and thermal to 450 keV for ^{60}Ni. The high resolution of the transmission data of Brusegan [20] permitted extension of the energy range for ^{60}Ni up to 800 keV. The experimental database used in the evaluation is displayed in Table VII. Details on the ORELA measurements of Perey indicated in Table VII can be found in Ref. [21] and [22]. The description of the experimental capture data of Guber *et al.* performed at ORELA is given in Ref. [23]. The direct capture cross sections were calculated from the direct-semi-direct capture model. Sets of evaluated resonance parameters and RPCM for each isotope were chosen to be obtained using the following steps.

1 In the SAMMY analysis of the experimental data, experimental parameters (EXP) for each experimental data set are determined via the Bayes fitting. Here EXP stands for data normalization, background corrections, and others. The first step consists of a sequential SAMMY analysis of the selected experimental database allowing the determination of the EXP. This procedure is made possible by using the code SAMAMR between each SAMMY sequence. A Complete Covariance Matrix (CCM) including the resonance parameters (RP) and the EXP, with their correlations, is obtained. The CCM could be used for the calculation of the combined statistical and systematic uncertainties of the calculated cross sections. However, such a matrix is not allowed in the ENDF format. After this analysis, a consistent experimental database is obtained by applying to each original experimental data set the resulting corrections.

2 A sequential SAMMY analysis of the consistent experimental database is performed; the initial values of the RP are those obtained from the adjustment in the first step. The EXP are not used. The RP and the RPCM are obtained, with variances and co-variances linked only to the statistical uncertainties of the experimental data. The RP should be very close to those obtained in the first step. This RPCM is suitable for the conversion to the ENDF format, but it does not contain the information con-

TABLE VII: Experimental database for the nickel isotopes.

Data Set	Ref.	Energy Range (keV)	Flight Path (m)	Density (at/b)
		^{58}Ni		
Transmission	[21]	0.1 - 53	78.217	0.0764
Transmission	[21]	53 - 180	78.217	0.0764
Transmission	[21]	180 - 813	201.578	0.1724
Capture	[23]	0.01 - 400	40.116	0.0364
Transmission	[20]	400 - 1000	387.760	0.0440
		^{60}Ni		
Transmission	[22]	1 - 200	78.203	0.0293
Transmission	[22]	1 - 200	78.203	0.0837
Transmission	[22]	20 - 450	78.203	0.0744
Capture	[23]	0.01 - 400	40.116	0.0360
Transmission	[20]	400 - 1000	387.760	0.0744

cerning the systematic uncertainties.

3 The Cross Section Covariance (CSCM) is calculated from the systematic uncertainties information obtained in step 1, completed by other information from authors and publications. The calculation of some uncertainties is straightforward, that is, the case for uncertainties due to normalization errors or background correction errors in neutron Time-Of-Flight (TOF) experiments. The uncertainties in multiple scattering corrections can be estimated by a fraction of the difference between the raw experimental data and the corrected data. It is estimated that SAMMY calculated the multiple scattering effect in capture cross sections with less than 10% error. The CSCMs are converted to ENDF format and are combined with the RPCM of step 2 for the calculation of the group cross-section uncertainties in the processing code PUFF-IV, or the NJOY/ERRORR [24]. The RPCM were used in the calculation of the uncertainty in the cross sections.

The thermal cross sections and their uncertainties calculated with the RPCM are shown in Table VIII for ^{58}Ni and ^{60}Ni, respectively. The reported uncertainties on the cross section are calculated as a combination of the RPCM and CSCM. Listed also in Table VIII are the ANR and VII.0 values. The covariance for the capture cross section in the resonance region for ^{58}Ni and ^{60}Ni are shown in Figs. 5 and 6, respectively. Also, covariances for elastic cross section for ^{58}Ni and ^{60}Ni are shown in Figs. 7 and 8, respectively. The calculations were done using the 44 groups of energy.

E. Chlorine ^{35}Cl and ^{37}Cl Resonance Evaluations Including Covariance

Resonance evaluations for ^{35}Cl and ^{37}Cl were carried out in the energy region from thermal to 1.2 MeV [25]. The expansion of the ENDF format with the LRF=7 option allowed inclusion of charged particle exit channels in the evaluation for ^{35}Cl. Since the proton exit channel for ^{35}Cl is open everywhere, that is, Q = +0.61522 MeV, the LRF=7 option for the resonance parameters was used. Also the compact formalism was used for covariance representation (LCOMP=1). The Reich-Moore format with LRF=3 was utilized for ^{37}Cl and LCOMP=1 for the covariance representation. The chlorine evaluations were based on fits of many data sets with the SAMMY code. A detailed discussion of the analysis methods used to determine parameter values and uncertainties are given in Ref. [25]. For capture and neutron width uncertainties, for example, for each resonance several SAMMY cal-

TABLE VIII: Nickel thermal cross sections and their uncertainties.

Isotope	Cross Section	VII.1	VII.0	ANR
^{58}Ni	Capture (b)	4.27±0.15	4.62	4.37±0.1
	Total (b)	29.32±0.48	29.64	29.67±0.5
	Scattering (b)	25.05±0.5	25.02	25.30±0.4
^{60}Ni	Capture (b)	2.40±0.06	2.76	2.50±0.06
	Total (b)	3.5±0.1	3.74	3.49±0.09
	Scattering (b)	1.1±0.03	0.98	0.98±0.07

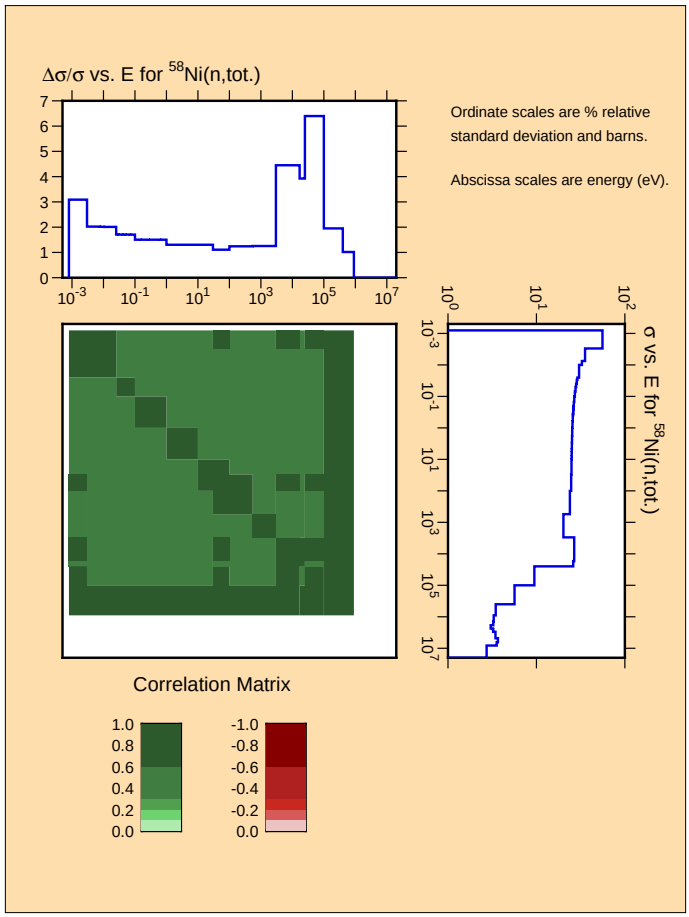

FIG. 5: Covariance for the ^{58}Ni total cross section in resolved resonance region.

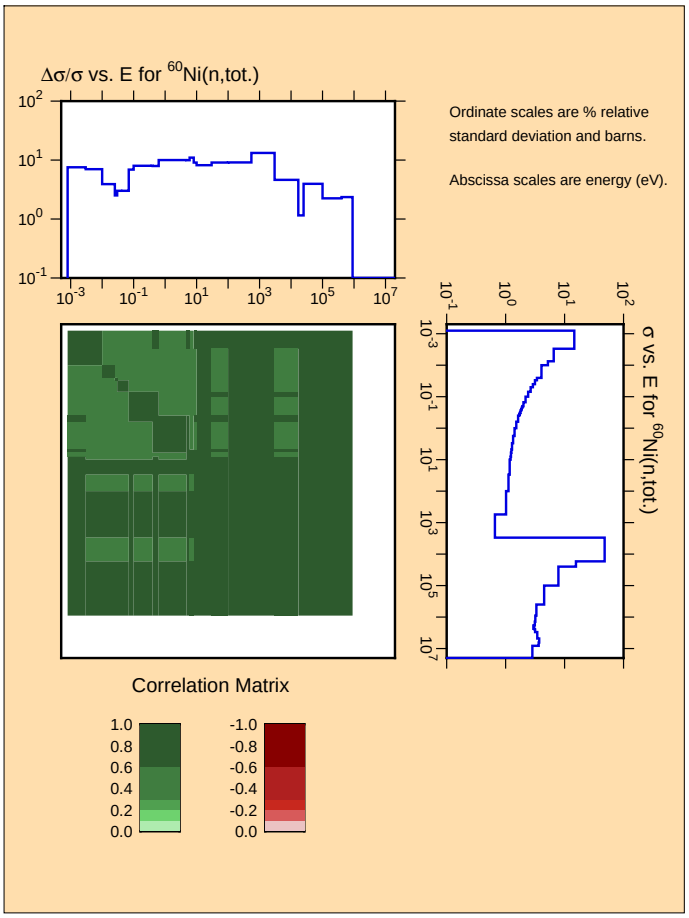

FIG. 6: Covariance for the ^{60}Ni total cross section in resolved resonance region.

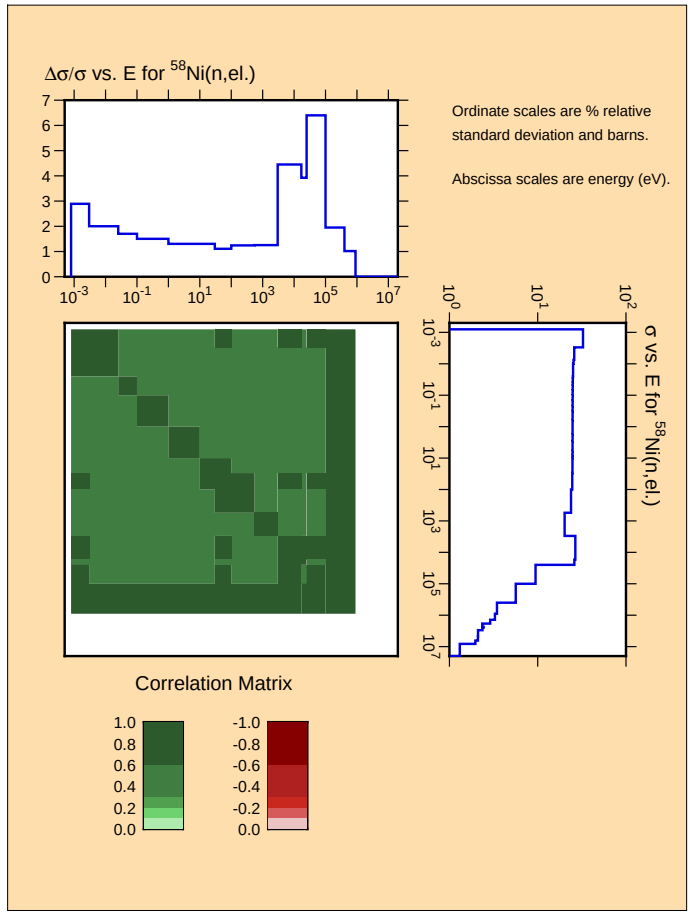

FIG. 7: Covariance for the ^{58}Ni scattering cross section in the resolved resonance region.

culations with different width values were overlaid with the data. Both the overlay plots and χ^2 changes with width variation were used to determine final uncertainties that were, in most cases, significantly larger than the SAMMY values. The RADCOP code [26] was used to generate both FILE2 and FILE32. At the time of the chlorine evaluation, SAMMY did not incorporate the now available "Prior Uncertainty Parameter", or PUP procedure. Thus, some normalization and background uncertainties were not propagated properly through the sequential analysis of multiple data sets. Although uncertainties in resonance energies and widths are felt to be realistic, the uncertainties in computed cross sections in valleys between resonances were underestimated. Furthermore, FILE32 is limited by the ENDF format to RP uncertainties and correlations, while uncertainties in nuclear radii cannot be treated directly. The "normalization/background/radius" effects were represented approximately by adjusting the FILE32 uncertainties for the external RPs and for selected resonances in the energy range of the evaluation. Since the resonance parameter representation does not include the direct capture (DC) part of the capture cross section, the DC component was included as a "background" $1/v$ cross section in FILE3, sections 1 and 102. At $E = 0.0253$ eV, the ^{35}Cl (^{37}Cl) DC cross section is 0.16 (0.31) b, which is a small (large) fraction of the overall capture cross section of 43.60 (0.433) b. The upper energy limit for the DC cross section is estimated to be 10 (100) keV for ^{35}Cl (^{37}Cl). The $1/v$ cross section was extended to 1.0 MeV to ensure continuity in the evaluation range. Guber *et al.* [27] describe in detail the DC calculations performed for ^{35}Cl and ^{37}Cl. It is shown that the $1/v$ cross section above 10 (100) keV are justifiable since the DC components are negligible compared to the resonance parameter contribution. Cross section at the thermal values for ^{35}Cl and ^{37}Cl calculated at room temperature are displayed on Table IX. The ^{35}Cl covariance of the (n,tot) reaction cross section is shown in Fig. 9. The covariance for the capture cross sections for ^{37}Cl is shown in Fig. 10. Note that due to the missing PUP option, in this case the systematic uncertainties were not incorporated properly and could lead to smaller uncertainties of the cross section.

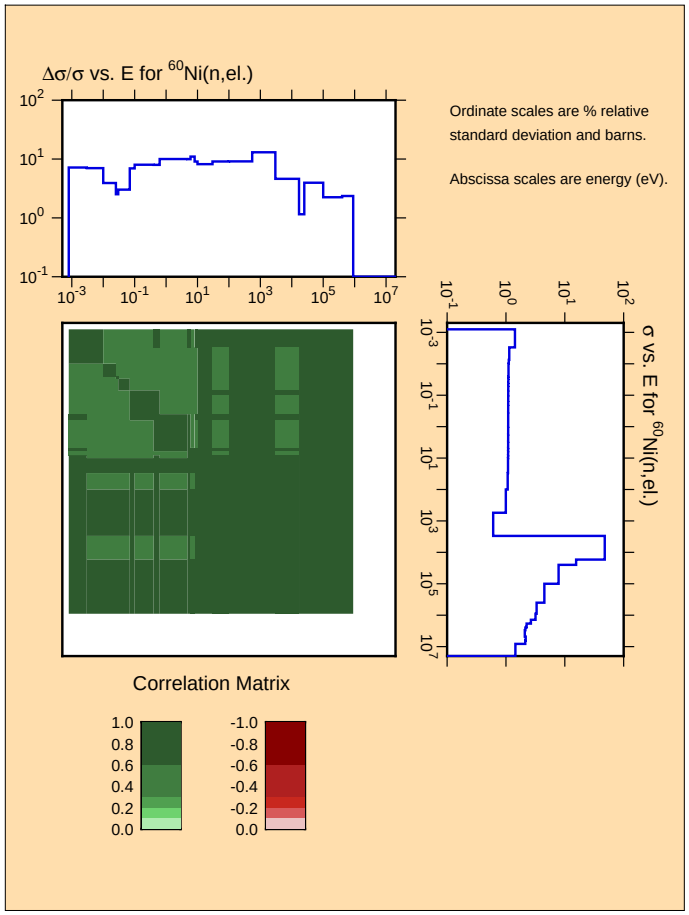

FIG. 8: Covariance for the ^{60}Ni scattering cross section in the resolved resonance region.

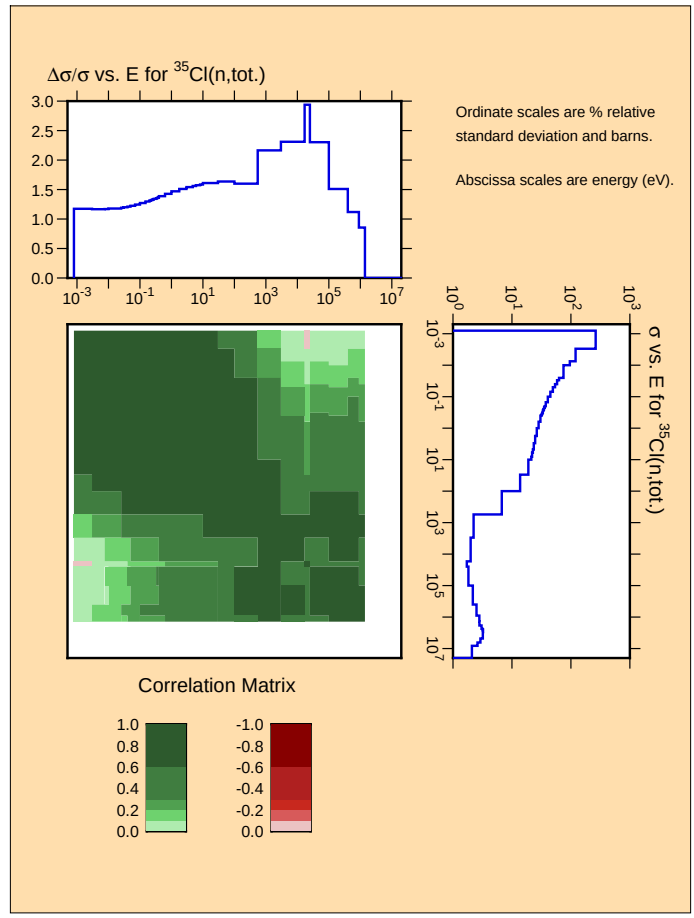

FIG. 9: ^{35}Cl covariance for the (n,tot) reaction cross section.

TABLE IX: Chlorine thermal cross sections and their uncertainties.

Isotope	Cross Section	VII.1	VII.0	ANR
^{35}Cl	Capture (b)	43.6±0.52	43.67	43.6±0.4
	Total (b)	64.8±0.7	65.12	64.7±0.5
	Scattering (b)	20.9±0.4	20.97	2.60±0.3
	(n,p) (b)	0.48±0.029	0.48	0.48±0.014
^{37}Cl	Capture (b)	0.433±0.006	0.433	0.433±0.006
	Total (b)	1.58±0.05	1.593	1.58±0.05
	Scattering (b)	1.15±0.05	1.16	1.15±0.05

F. Potassium ^{39}K and ^{41}K Evaluations Including Covariance

We performed an evaluation of ^{39}K and ^{41}K neutron cross section in the resolved resonance region with the multilevel Reich-Moore R-matrix formalism. The evaluation incorporates recent high-resolution capture and transmission measurements made at ORELA to extend the resolved resonance energy range up to 1.0 MeV with much more accurate representation of the data than previous evaluations. The data included transmission measurements by Guber *et al.* [28] and Good et al. [29] on the 80-m flight path at ORELA; total cross section data of Cierjacks *et al.*[30] on a 57-m flight path performed at the Karlsruhe Isochronous Cyclotron; and measurements of Singh *et al.*[31] done at the 200-m flight path at the Columbia synchrocyclotron. Also included in the evaluation were the high-resolution capture cross sections of Guber *et al.* [28] measured in the energy range of 0.1 keV to 600 keV and an older low resolution capture data of Joki et al. [32] done in the energy region from 0.02 eV to 10 eV. We have included RPs in FILE2, MT=151,and the corresponding RPCM in FILE32, MT=15. The Reich-Moore format with LRF=3 and LCOMP=1 was utilized. The applicable energy range is 10^{-5} eV to 1.0 MeV. The RADCOP code was used to generate both FILE2 and FILE32. At 1.0 MeV the FILE3 total and elastic cross section values for the previous ENDF evaluations were adjusted slightly to join smoothly with the resonance parameter values. For capture cross sections above 1 MeV, the previous ENDF ^{39}K theoretical values were normalized to 0.436 mb at 1 MeV, and the ^{41}K values were normalized by a factor of 0.594 to match the data of Ref. [33] at 1 MeV. Since the resonance parameter representation does not include the direct capture (DC) part of the capture cross section, the DC component was included as a "background" $1/v$ cross section in File 3, sections 1 and

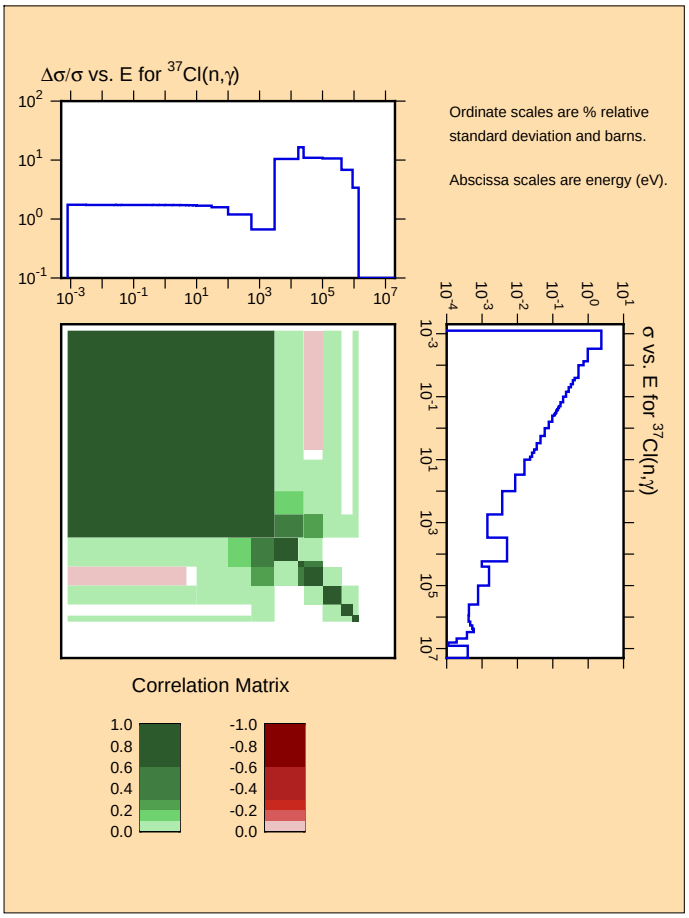

FIG. 10: Covariance for the capture cross section of ^{37}Cl.

102. At E = 0.0253 eV, the calculated DC cross section for ^{39}K (^{41}K) is 0.80 (0.52) b, which is a large fraction of the overall thermal capture cross section of 2.10 (1.46) b. The upper energy limit for the DC cross section is estimated to be 100 keV. Therefore, the "background" $1/v$ cross section was terminated at this energy value. The Table X gives a comparison of the thermal elastic, capture and total cross sections at room temperature with the data listed in ANR. Also shown in Table X are the thermal values calculated with VII.0. The quoted uncertainties, obtained from File 32, reflect the rather large experimental uncertainties in the thermal values. The thermal scattering cross section for ^{41}K in the ANR is almost 3 times smaller than that of the present evaluation. The reasons for this discrepancy are not understood, but we would like to point out that we are in agreement with previous evaluations. The covariance for the capture cross sections for ^{39}K and ^{41}K are shown in Fig. 11 and Fig. 12, respectively.

G. Manganese ^{55}Mn Resonance Evaluation

Accurate neutron capture cross sections of ^{55}Mn are important for reactor designs in view of its use as alloy structural material. Manganese as a constituent of stainless steel is present in operations and processing involving fissile material, and accurate cross section data are needed to support criticality safety analyses. Resonance parameters for ^{55}Mn in the VII.0-evaluated data files are mainly based on the work performed by Garg *et al.* [34] and by Macklin [35]. The work by Macklin was aimed to meet the "World Request of Nuclear Data" (WRENDA) of 10% accuracy in the lowest energy resonances and 20% accuracy up to 100 keV. Measurements done by Perrot et al. [36] using a lead slowing-down spectrometer and simulation have shown that the ^{55}Mn-evaluated capture cross sections are inadequate in the energy range of 50 eV to 30 keV. A suggestion was made to reevaluate the ^{55}Mn

TABLE X: Potassium thermal cross sections and their uncertainties.

Isotope	Cross Section	VII.1	VII.0	ANR
^{39}K	Capture (b)	2.13±0.1	2.1	2.1±0.2
	Total (b)	4.19±0.14	4.19	-
	Scattering (b)	2.06±0.1	2.09	1.99±0.17
^{41}K	Capture (b)	1.46±0.09	1.46	1.46±0.03
	Total (b)	4.03±0.14	4.06	-
	Scattering (b)	2.56±0.1	2.6	0.92±0.2

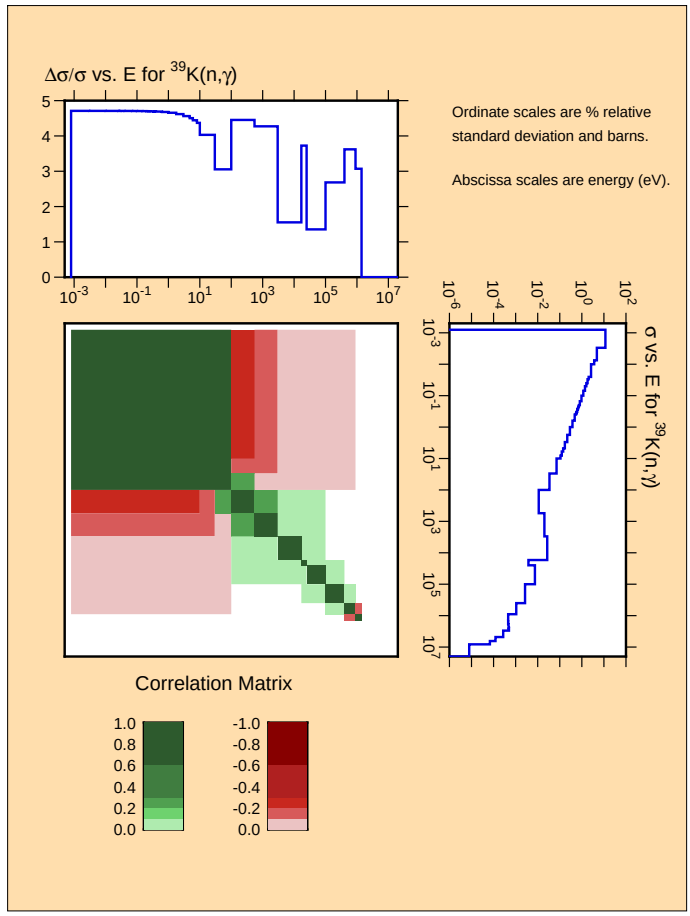

FIG. 11: Covariance for the capture cross section of ^{39}K.

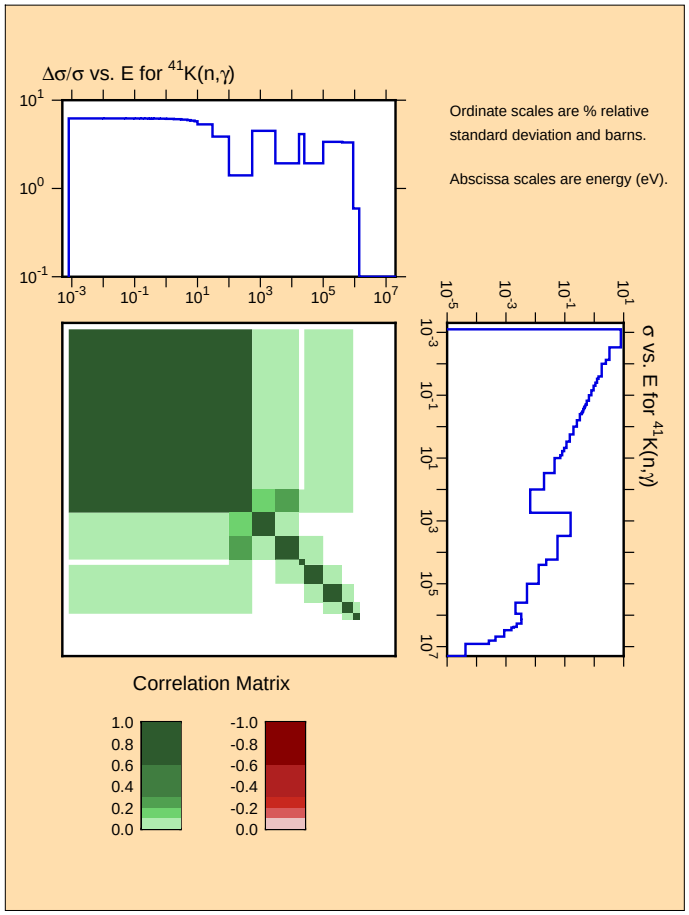

FIG. 12: Covariance for the capture cross section of ^{41}K.

cross section [37]. For that reason a new resonance evaluation of ^{55}Mn was carried out with the SAMMY code including recent experimental transmission and capture data measured at ORELA and GELINA facilities. The evaluation was done in attempt to obtain more accurate resonance parameters in the energy range from thermal to 125 keV, below the first inelastic channel. The experimental database includes the 1988 neutron transmission of Harvey *et al.* [38], the 2005 GELINA capture cross section measurement of Schillebeeckx *et al.* [39] and the ORELA capture measurement of Guber *et al.* [40]. The experimental resolution of the capture data allowed a good separation of the resonances up to 125 keV neutron energy. For the evaluation of the cross sections in the thermal energy range, earlier measurements were added to the experiment database: total cross section from Cote *et al.* [41] and Rainwater *et al.* [42] and capture cross section from Widder *et al.* [43]. The database used in the evaluation is shown in Table XI.

It is noted that the accuracy of the parameters has improved compared to that of the VII.0 evaluation. The infinite dilute capture resonance integral calculated from the ^{55}Mn VII.1 evaluation is 13.52±0.3 b compared to 13.4±0.5 listed in the ANR and 13.42 from VII.0. The ^{55}Mn thermal cross sections and uncertainties are displayed on Table XII including the thermal values of the ANR and for the VII.0. Covariances for the ^{55}Mn capture cross section are shown in Fig. 13.

TABLE XI: New experimental data for ^{55}Mn included in the evaluation.

Data Set	Ref.	Energy Range (keV)	Flight Path (m)	Density (at/b)
		^{55}**Mn**		
Transmission	[38]	3 - 125	80.117	0.0416
Capture	[39]	0.01 - 125	58.586	0.0190
Capture	[40]	0.01 - 125	40.411	0.0178

TABLE XII: Manganese thermal cross sections and their uncertainties.

Cross Section	VII.1	VII.0	ANR
Capture (b)	13.27±0.11	13.41	13.36±0.05
Total (b)	15.39±0.2	15.58	-
Scattering (b)	2.12±0.04	2.17	2.06±0.03

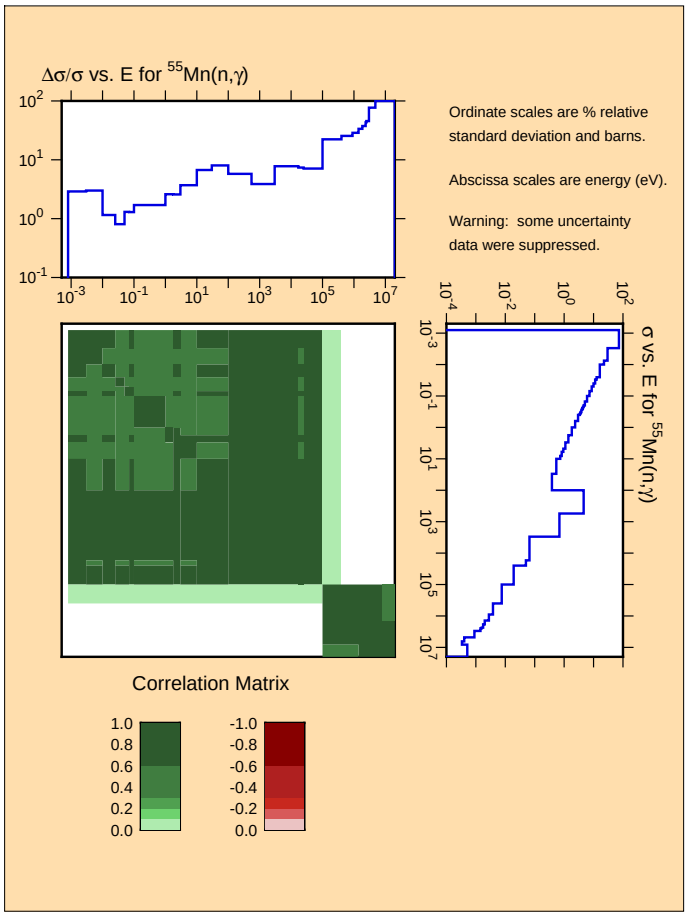

FIG. 13: Covariance for the capture cross section of ^{55}Mn.

IV. COVARIANCE EVALUATION FOR MAJOR ACTINIDES

This section gives a short description of the technique used for covariance generation of ^{233}U, ^{235}U, ^{238}U, and ^{239}Pu. A more detailed description of the methodologies used can be found in Ref. [44].

A. Covariance Evaluations for ^{233}U

The resonance evaluation for ^{233}U has been performed in the energy range 0 to 600 eV using the Reich-Moore formalism of the computer code SAMMY [45]. The description of the resolved cross section encompassed a total of 769 resonances including the external levels with a RPCM. However, this matrix is no longer available; therefore, the retroactive approach was used to generate RPCM. The Reich-Moore formalism for each resonance is described by five parameters (the resonance energy E_r, the gamma width Γ_γ, the neutron width Γ_n, and the two fission widths Γ_{f1} and Γ_{f2}), which total to 3845 parameters. This large number of resonance parameters leads to problems for the data storage for the resulting covariance file. It was addressed at ORNL by the development of a methodology to convert FILE32 into FILE33 representation [46]. The resulting reduction in storage permitted the processing of the covariance data and production of covariance matrices for groupwise cross sections used by the processing codes.

Twenty-eight energy groups of the SCALE 44-group structure describe the energy region below 600 eV. The correlation matrix for the group fission cross section is shown in Fig.14. Below 1 eV the group fission cross sections are highly correlated. The jump in uncertainties is an artifact of the binning of the data and more importantly the joining of resolved resonance region and the unresolved resonance region. The thermal cross sections and uncertainties are listed in Table XIII.

TABLE XIII: Thermal cross sections for ^{233}U and their uncertainties.

Cross Section	VII.1	ANR
Capture (b)	45.25±0.91	45.5±0.7
Total (b)	588.65±2.21	587.5±1.0
Scattering (b)	12.18±0.65	12.7±0.3
Fission (b)	531.22±1.51	529.1±1.2

B. Covariance Evaluations for ^{235}U

The Reich-Moore resonance evaluation has been performed in the energy range 0 to 2250 eV [47] with a total of 3193 resonances, including the external levels. Since the RPCM generated no longer existed, the retroactive approach was used [48] for a total of 15965 parameters. This led to a RPCM in the ENDF/B format using 1.76 Gigabytes. With changes to the PUFF-IV code, the processing time of the covariance data was reduced significantly. A great reduction in processing time was achieved. More details of the computation can be found in Ref. [44].

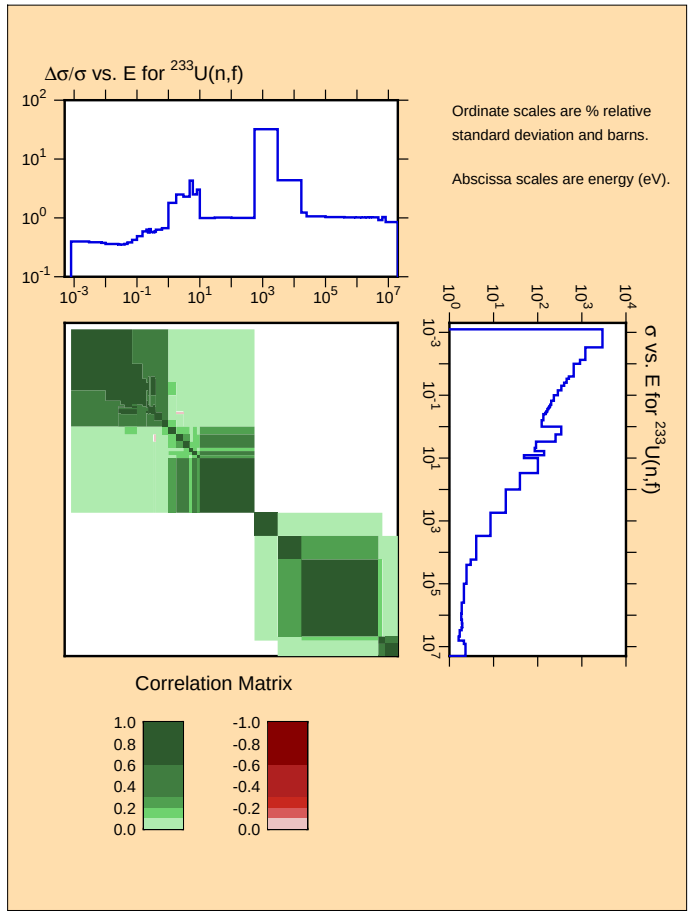

FIG. 14: Group cross section correlations for the fission cross section of ^{233}U.

The capture cross section covariance data processed with PUFF-IV code in the 44-group structure are shown in Fig. 15 with an average uncertainty of about 1% up to 1 keV. It appears that the 1% uncertainty in the thermal capture cross section has influenced the correlation of the resolved resonance energy region. The covariance for the fission cross section is shown in Fig. 16. The uncertainty in the thermal fission cross section is less than 0.2% in good agreement with the standard values. As for ^{233}U, the jump in uncertainties is an artifact of the binning of the data and more importantly the joining of resolved resonance region and the unresolved resonance region. The covariance evaluations for the cross section above 2250 eV and for the number of neutrons per fission ($\bar{\nu}$) were done at Los Alamos National Laboratory [49]. The thermal cross sections and uncertainties are listed in Table XIV together with the ANR values.

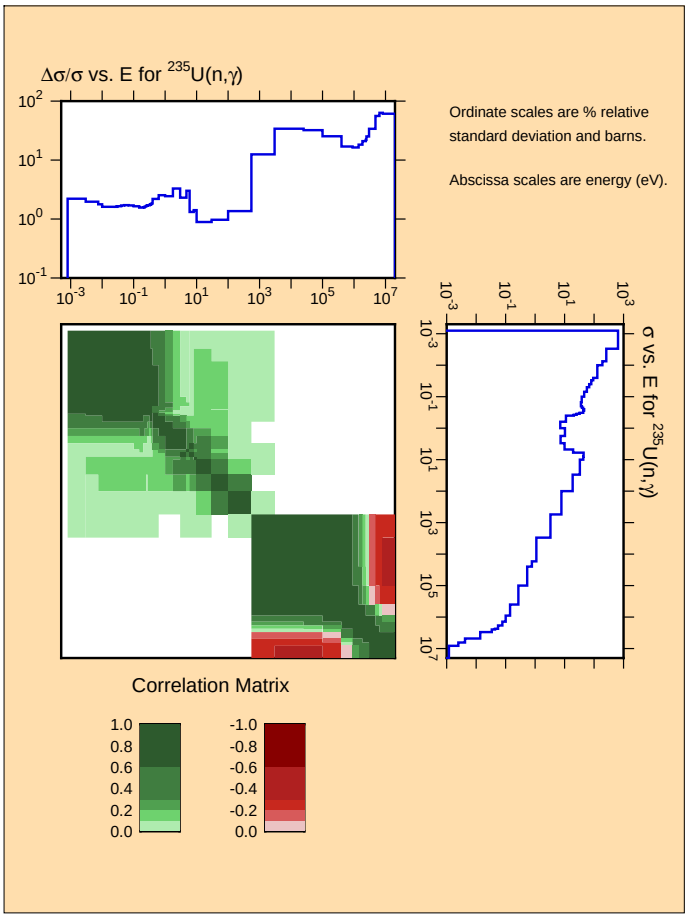

FIG. 15: Correlation matrixes for the ^{235}U capture cross section in the 44-neutron energy group structure.

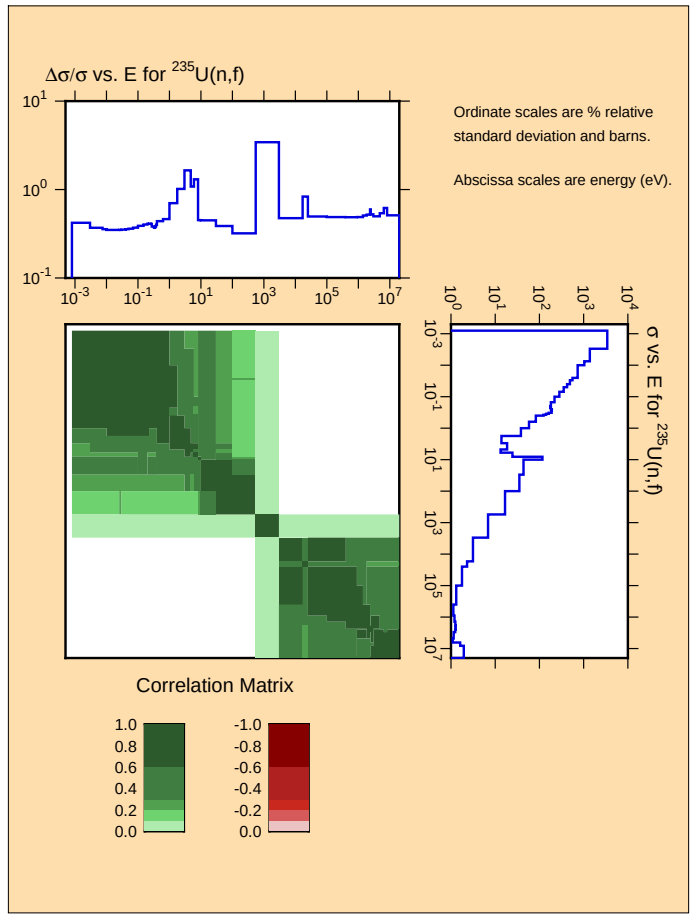

FIG. 16: Correlation matrixes for the ^{235}U fission cross section in the 44-neutron energy group structure

TABLE XIV: Thermal cross sections for ^{235}U and their uncertainties.

Cross Section	VII.1	ANR
Capture (b)	98.67±1.58	98.8±0.8
Total (b)	698.68±1.79	694.8±1.2
Scattering (b)	15.11±0.77	14.02±0.22
Fission (b)	584.9±2.0	582.6±1.1

TABLE XV: ^{238}U thermal cross sections and their uncertainties.

Cross Section	VII.1	ANR
Capture (b)	2.68±0.05	2.680±0.019
Scattering (b)	9.31±0.08	9.075±0.015

C. Covariance Evaluations for ^{238}U

A detailed description of the cross section evaluation for ^{238}U can be found in Ref.[50], which resulted in 3312 resonances in the energy range from 0 to 20 keV. With the 22 negative-energy resonances, and 9 resonances above 20 keV, a total of 3343 resonances describe the resolved resonance region. The fission cross section is negligible below 20 keV; therefore, each resonance of can be described by only three parameters: the resonance energy E_r, the gamma width Γ_γ, and the neutron width Γ_n. The experimental uncertainties were incorporated directly into the evaluation process, including statistical and systematic uncertainties for each of the differential data sets plus the quoted uncertainties for the resonance integral and thermal cross section. The result is a complete RPCM associated with the set of parameters of 800 megabytes in size. Results from PUFF-IV processing were cross-checked with results obtained from a similar calculation by SAMMY; no major differences were found. Capture cross section correlations for the 44-neutron energy groups are shown in Fig. 17. Uncertainties in the capture cross section in the resonance region (up to 20 keV) range from 1 to 4%. Above 20 keV the uncertainty can be as high as 25%. Thermal values are listed in Table XV.

D. Covariance Evaluations for ^{239}Pu

The resolved resonance evaluation from 0 to 2500 eV is described in Ref. [51]. With a single SAMMY run includ-

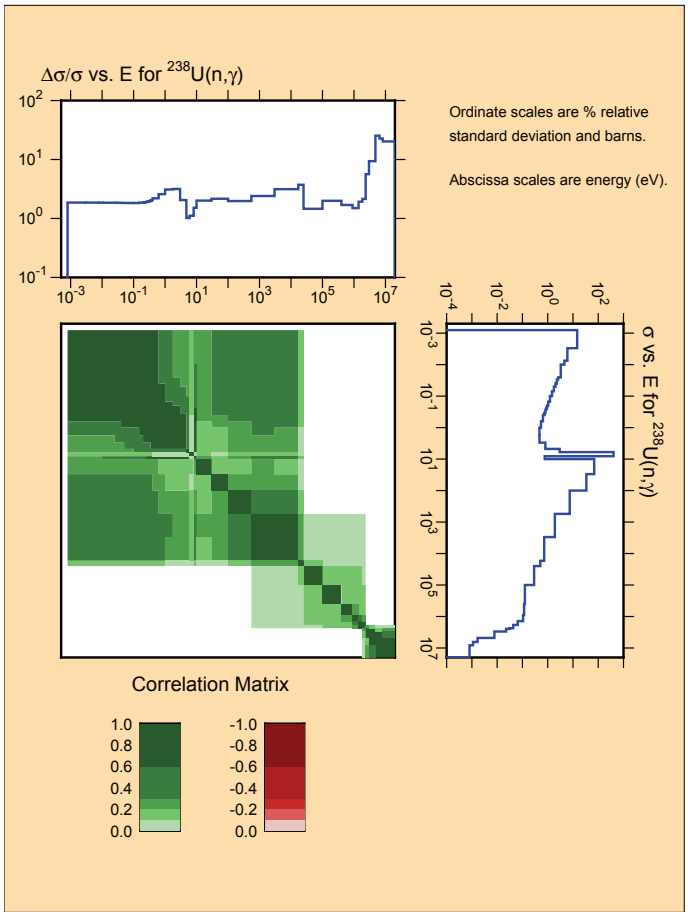

FIG. 17: Correlation matrices for the ^{238}U capture cross section in the 44-neutron energy group structure.

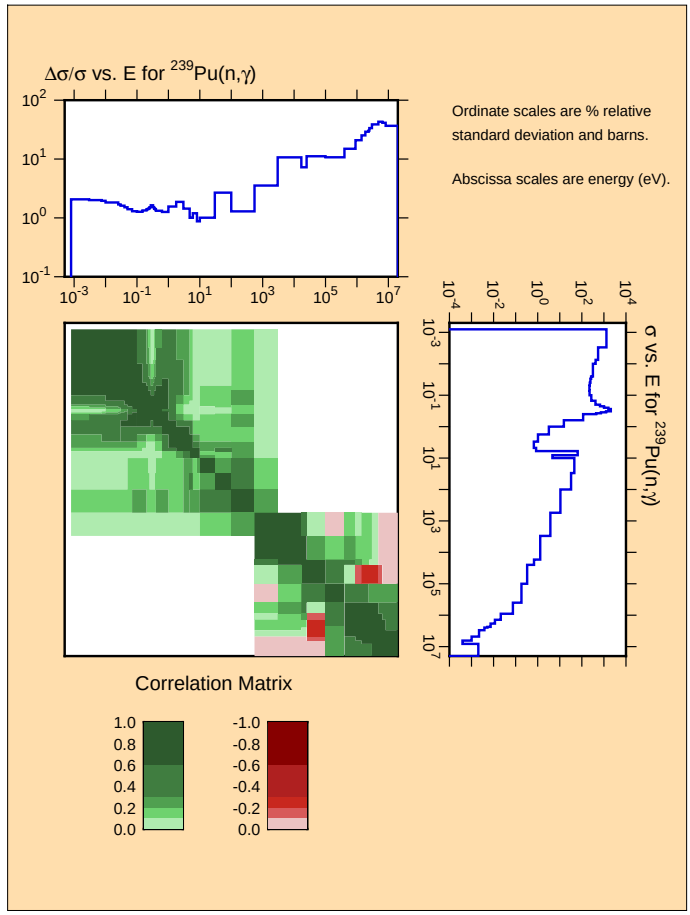

FIG. 18: Correlation matrices for the ^{239}Pu capture cross section in the 44-neutron energy group structure.

ing all the experimental data, the RPCM was obtained. No data set covering the entire energy range of the resonances existed at the time of the evaluation; therefore, the RPCM was derived based on "experimental" fission and capture cross sections generated in the energy range 0 to 2500 eV from the resonance parameters. The RPCM was converted into the FILE33 CSCM, which led to a file of 140 kilobytes. The capture and fission cross section correlations are shown in Fig. 18 and Fig. 19, respectively. The covariance evaluation above 2500 keV was performed at LANL[49]. The uncertainty of the capture cross section in the resonance region varies between 2 and 10%, whereas above 2500 eV it can be as high as 40%. The covariance data was used in a benchmark calculation as shown in Ref.[52]. Thermal values are listed in Table XVI. The reason why the thermal uncertainties are much larger than the uncertainties quoted in the ANR is unknown.

E. Benchmark Calculations and Data Uncertainty

To illustrate the impact of nuclear data uncertainty and covariance in benchmark calculations, thermal benchmark system calculations have been carried out for integral experiments with uranium isotopes as part of it. The benchmark experiment for which the uncertainty in the multiplication factor (k_{eff}) was investigated is the LEU-SOL-THERM-002 case 1 included in the International Criticality Safety Benchmark Evaluation Project (ICSBEP) [53]. The experiments consist of a series of critical measurements performed in the 1950s at the Oak Ridge National Laboratory with low-enriched uranium (4.9 wt. % ^{235}U). The system sensitivity of k_{eff} to the ^{235}U fission cross-section, capture cross section, and $\bar{\nu}$ are shown in Fig. 20. Also shown in Fig. 20 is the sensitivity of the k_{eff} to the ^{238}U capture cross section. As can be seen, the k_{eff} of this thermal benchmark system is very sensitive to the ^{235}U and ^{238}U nuclear data. The sensitiv-

TABLE XVI: Thermal cross sections for ^{239}Pu and their uncertainties.

Cross Section	VII.1	ANR
Capture (b)	270.5±4.9	269.3±2.9
Total (b)	1026.5±7.8	1025.3±2.9
Scattering (b)	7.97±0.17	7.94±0.36
Fission (b)	748.0±5.5	748.1±2.0

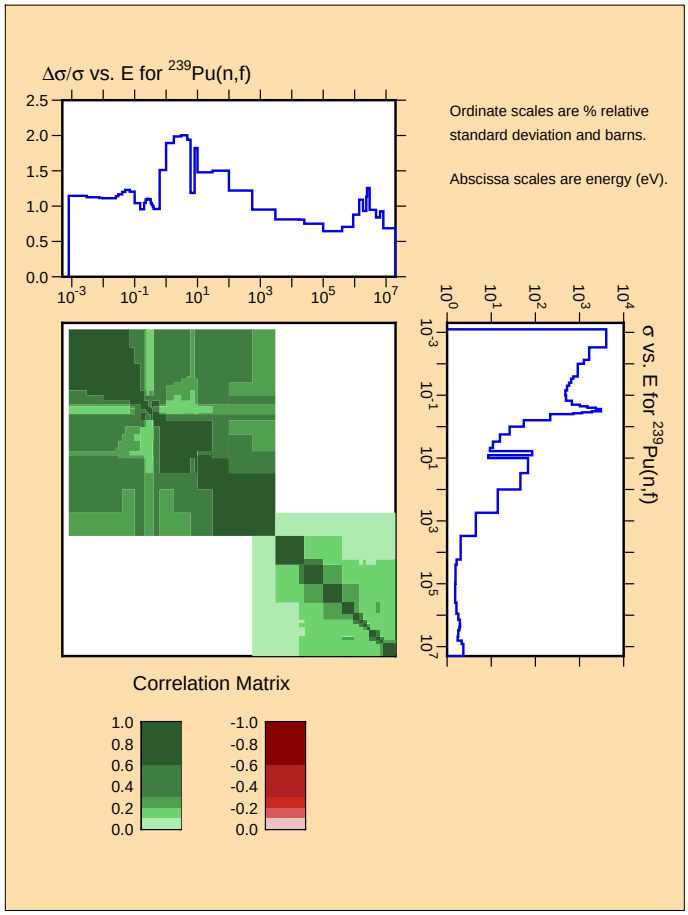

FIG. 19: Correlation matrices for the ^{239}Pu fission cross section in the 44-neutron energy group structure.

ity S of the calculated multiplication factor to the cross section is defined as

$$S = \frac{p}{k_{eff}} \frac{\partial k_{eff}}{\partial p}, \tag{3}$$

where k_{eff}, as before, is the calculated multiplication factor, and p is the nuclear data parameter, as for instance the fission cross section σ_f.

The k_{eff} benchmark calculations were done with the TSUNAMI code [54] that performs automated multi-group cross section processing followed by a forward and adjoint neutron fluxes calculation based on the KENOV.a Monte Carlo code [55]. The calculations were done using the SCALE [56] 238-group cross section based on the ENDF/B-VII.0. For the uncertainty calculations, the covariance data were generated with the PUFF-IV code in the COVERX format based on the SCALE 44-group library. Except for ^{235}U and ^{238}U, which were replaced in the 238-group and 44-group libraries, the SCALE libraries were used in the benchmark calculations. Results of calculations with TSUNAMI give a k_{eff} of 1.0004±0.0003. The quoted uncertainty is due to the stochastic aspect of the Monte Carlo calculation. The nuclear data uncertainty was propagated with the

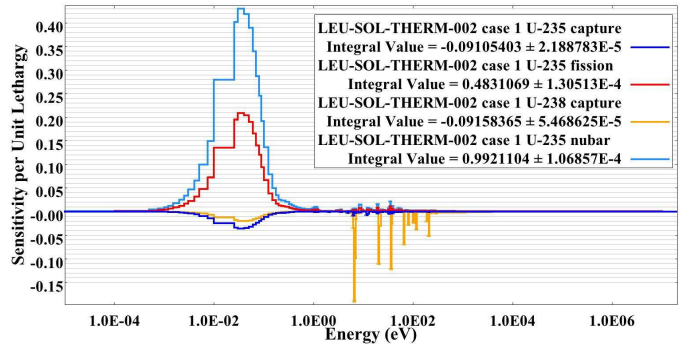

FIG. 20: Sensitivity of the k_{eff} to the capture and fission cross section and $\bar{\nu}$ for ^{235}U. Also shown is the sensitivity of k_{eff} to the ^{238}U capture cross section.

TSUNAMI code to the final k_{eff}. The total percentage uncertainty in the calculated k_{eff} due to all isotopes present in the benchmark experiment is 0.5335±0.0001. The percentage contributions of the uncertainty in k_{eff} due to the nuclear data of ^{235}U and ^{238}U are shown in Table XVII and Table XVIII, respectively. As can be seen in these tables, the largest uncertainty for ^{235}U is due to the number of neutrons per fission ($\bar{\nu}$) whereas for ^{238}U the uncertainty in the capture cross section dominates. It is also noted from Table XI that the uncertainty in the fission spectrum (χ) for ^{235}U is important. The values in these tables, positive and negative, indicate the data are correlated and uncorrelated, respectively. The total uncertainty is obtained by squaring each value indicated in the Table and adding (correlated data) or subtracting (uncorrelated data). By doing so, the calculated percentage uncertainty in k_{eff} due to the ^{235}U and ^{238}U nuclear data are, respectively, 0.4488±0.0001 and 0.1375±0.0001. The combined ^{235}U and ^{238}U uncertainty is 0.4694±0.0001. It is worth noting that ^{235}U and ^{238}U data uncertainty contribution to the total uncertainty is about 88%. These results demonstrate the importance of the ^{235}U and ^{238}U data uncertainties in determining safety margin in k_{eff} calculations.

V. SUMMARY AND CONCLUSIONS

This paper describes the methodologies used at ORNL to generate resonance parameter covariance data using the computer code SAMMY. Covariance data were generated for the chromium isotopes, titanium isotopes, ^{19}F, ^{35}Cl, ^{37}Cl, ^{39}K, ^{41}K, ^{55}Mn, ^{58}Ni, ^{60}Ni, ^{233}U, ^{235}U, ^{238}U, and ^{239}Pu. ORNL has developed alternatives to address concerns with the size of the covariance data. The large size of the covariance matrix will not be a problem since the option of translating the ENDF covariance from the FILE32 into the FILE33 or compact representation (LCOMP = 2) leads to a great reduction in computer storage without loosing the features inherent in the

TABLE XVII: Contribution to the uncertainty in k_{eff} by individual components or cross correlations of the ^{235}U nuclear data, units of $\%\delta k/k$.

Isotope	Reaction	Reaction	Correlation Values
^{235}U	$\bar{\nu}$	$\bar{\nu}$	$3.0497\times10^{-1}\pm6.8935\times10^{-6}$
	χ	χ	$2.0341\times10^{-1}\pm1.7216\times10^{-5}$
	(n,f)	(n,f)	$1.6832\times10^{-1}\pm5.2006\times10^{-6}$
	(n,γ)	(n,γ)	$1.4094\times10^{-1}\pm3.3711\times10^{-6}$
	(n,f)	(n,γ)	$1.3729\times10^{-1}\pm2.3744\times10^{-6}$
	(n,n)	(n,f)	$-1.8158\times10^{-3}\pm2.1364\times10^{-7}$
	(n,n)	(n,γ)	$1.5671\times10^{-3}\pm1.1139\times10^{-7}$
	(n,n')	(n,n')	$6.3581\times10^{-4}\pm7.5642\times10^{-10}$
	(n,n)	(n,n')	$-3.5289\times10^{-4}\pm2.5432\times10^{-10}$
	(n,n)	(n,n)	$1.4231\times10^{-4}\pm1.2089\times10^{-10}$
	$(n,2n)$	$(n,2n)$	$8.5166\times10^{-5}\pm2.1360\times10^{-11}$
	(n,n)	$(n,2n)$	$-1.1576\times10^{-5}\pm3.4023\times10^{-12}$

TABLE XVIII: Contribution to the uncertainty in k_{eff} by individual components or cross correlations of the ^{238}U nuclear data, units of $\%\delta k/k$.

Isotope	Reaction	Reaction	Correlation Values
^{238}U	(n,γ)	(n,γ)	$1.2611\times10^{-1}\pm6.9011\times10^{-6}$
	(n,n')	(n,n')	$4.6681\times10^{-2}\pm3.9224\times10^{-6}$
	(n,n)	(n,n)	$2.7686\times10^{-2}\pm3.8012\times10^{-6}$
	(n,n)	(n,n')	$-2.3038\times10^{-2}\pm1.1567\times10^{-6}$
	(n,n)	(n,γ)	$2.2160\times10^{-2}\pm3.9885\times10^{-6}$
	$\bar{\nu}$	$\bar{\nu}$	$9.1769\times10^{-3}\pm8.0248\times10^{-9}$
	$(n,2n)$	$(n,2n)$	$3.1500\times10^{-3}\pm1.2132\times10^{-9}$
	(n,f)	(n,f)	$2.8047\times10^{-3}\pm1.2132\times10^{-9}$
	χ	χ	$1.9456\times10^{-3}\pm1.5780\times10^{-9}$
	(n,n)	$(n,2n)$	$-4.0115\times10^{-4}\pm3.2520\times10^{-9}$
	(n,f)	(n,γ)	$3.9167\times10^{-4}\pm1.4057\times10^{-10}$
	(n,n)	(n,f)	$-3.8047\times10^{-4}\pm2.9636\times10^{-10}$

FILE32. While computer speed and storage have constantly been improving, it is worthwhile to have small sized data evaluations. The evaluations are stored in nuclear data banks and are retrieved by users worldwide who may have limited network and processing capabilities to download and process the data. The covariance data have been processed with the PUFF-IV code to obtain group cross section uncertainty data on any user-defined neutron group structure. In particular, the calculations presented here are for the 44-group structure of the SCALE system. The covariance data were used in sensitivity calculations to assess the uncertainty in k_{eff} for thermal, intermediate-energy, and fast-energy benchmark systems. The evaluated covariance data presented in this work will be part of the ENDF/B-VII release 1.

Acknowledgments

ORNL is managed by UT-Battelle, LLC, under contract DE-AC05-00OR22725 with the U.S. Department of Energy. This work was sponsored by the U.S. Department of Energy Nuclear Criticality Safety Program.

[1] N. M. Larson, "Updated Users' Guide for SAMMY: Multilevel R-Matrix Fits to Neutron Data Using Bayes Equations," Oak Ridge National Laboratory, ORNL/TM-9179/R8 (2008).

[2] M. B. Chadwick *et al.*, "ENDF/B-VII.1 Evaluated Nuclear Data for Nuclear Science and Technology. Part 1: Neutron Cross Sections and Fission Product Yields," Nuclear Data Sheets 112, 2887 (2011).

[3] S.Y. Oh and L.C. Leal,"SUGGEL: A Program Suggesting the Orbital Angular Momentum of a Neutron Resonance from the Magnitude of its Neutron Width,"Oak Ridge National Laboratory, ORNL/TM-2001/314 (2001).

[4] R.O. Sayer,"RSAP- A Code for Display of Neutron Cross Section Data and SAMMY Fit Results," Oak Ridge National Laboratory, ORNL/TM-2001/15 (2001).

[5] D. Wiarda, S. Goluoglu, M. E. Dunn, N. M. Greene, and L. M. Petrie, "AMPX-6: A Modular Code System for Processing ENDF/B Evaluations," To be published as an Oak Ridge National Laboratory ORNL/TM Report.

[6] D. Wiarda and M. E. Dunn, "PUFF-IV: A Code for Processing ENDF Uncertainty Data into Multigroup Covariance Matrices," Oak Ridge National Laboratory, ORNL/TM-2006/147 (2006).

[7] L. Leal, H. Derrien, K. Guber, G. Arbanas, and D. Wiarda, "Evaluation of the Chromium Resonance Parameters Including Resonance Parameter Covariance," International Conference on Nuclear Data for Science and Technology, April 26 - 30, 2010, Jeju Island, Korea, Journal of the Korean Physical Society, 59, 1644 (2011)

[8] K. H. Guber, P. E. Koehler, D. Wiarda, J. A. Harvey, T. S. Bigelow, C. Ausmus, D. R. Brashear, and J. A. White, "New Neutron-induced Cross Section Measurements for Improved Nuclear Data," International Conference on the Physics of Reactors Nuclear Power: A Sustainable Resource Casino-Kursaal Conference Center, Interlaken, Switzerland, September 14 - 19, 2008.

[9] J. Harvey Transmission Data for Chromium Isotopes, Private Communication.

[10] S. F. Mughabghab, "Atlas of Neutron Resonances Resonance Parameters and Thermal Cross Sections Z=1-100," Elsevier, Amsterdam 2006.

[11] L. Leal, K. Guber, G. Arbanas, D. Wiarda, and P. Koehler, "Resonance Evaluation of ^{48}Ti Including Covariance for Criticality Safety Applications," Proceedings

of the International Conference on Nuclear Criticality, September 19 - 23, 2011, Edinburgh, Scotland.

[12] K. H. Guber, P. E. Koehler, D. Wiarda, and J. A. Harvey, "Neutron Cross-Section Measurements on Structural Materials at ORELA," International Conference on Nuclear Data for Science and Technology, April 26 - 30, 2010, Jeju Island, Korea, Journal of the Korean Physical Society, 59, 1685 (2011).

[13] L. C. Leal and H. Derrien, "R-Matrix Evaluation of ^{19}F Neutron Cross Section up to 1 MeV," Transaction of the American Nuclear Society, page 494, June 1 - 5, 2003, San Diego California.

[14] D. C. Larson, C. H. Johnson, J. A. Harvey, and N. W. Hill, "Measurement of the Neutron Total Cross Section of Fluorine from 5 eV to 20 MeV," Oak Ridge National Laboratory, ORNL/TM-5612 (1976).

[15] K. H. Guber, L. C. Leal, R. O. Sayer, P. E. Koehler, T .E. Valentine, H. Derrien and J. A. Harvey, PHYSOR 2004 , "The Physics of Fuel Cycles and Advanced Nuclear Systems: Global Developments," Chicago, Illinois, April 25 - 29, 2004.

[16] D. L. Broder, A. F. Gamalii, A. I. Lashuk, and I. P. Sadokhin, "The (n,n′)-Reaction of Fluorine, Iron, Cobalt, Nickel, and Tantalum," Proceedings of the Second International Conference on Nuclear Data for Reactors, Helsinki, Finland, 1970 (International Atomic Energy Agency, Vienna, Austria, 1970).

[17] L. J. Rainwater, W. W. Havens, Jr., J. R. Dunning, and C. S. Wu, "Slow Neutron Velocity Spectrometer Studies of H, D, F, Mg, S, Si, and Quartz," Phys. Rev. Vol 73, 733 (1948).

[18] S. Raman, E. K. Warburton, J. W. Starner, E. T. Jurney, and J. E. Lynn, Spectroscopy of ^{20}F Levels, Phys. Rev. C, 53, 626 (1996).

[19] H. Derrien, L. C. Leal, K. H. Guber, D. Wiarda, and G. Arbanas, "Re-evaluation of ^{58}Ni and ^{60}Ni resonance parameters in the neutron energy range thermal to 800 keV," Wonder 2009 - 2nd International Workshop on Nuclear Data Evaluation for Reactor Applications, Cadarache, France, 2009.

[20] A. Brusegan, G. Rohr, R. Shelley, E. Macavero, C. van der Vorst, F. Poortmans, L. Mewissen, G. Vanpraet, "Very High Resolution Transmission Measurements and Resonance Parameters for ^{58}Ni and ^{60}Ni," Proc. Int. Conf. on Nuclear Data for Science and Technology, Gatlinburg, Tenn., 1994, p. 224. ANS, 1994.

[21] C. M. Perey, F. G. Perey, J. A. Harvey, N. W. Hill, N. M. Larson, and R. L. Macklin, "^{58}Ni + n Transmission, Differential Elastic Scattering and Capture Measurements and Analysis from 5 to 813 keV," Oak Ridge National Laboratory, ORNL/TM-10841; ENDF-347 (1988).

[22] C. M. Perey, J. A. Harvey, R. L. Macklin, R. R. Winters, and F. G. Perey, "Neutron Transmission and Capture Measurements and Analysis of ^{60}Ni from 1 to 450 keV," Oak Ridge National Laboratory, ORNL/TM-5899 (1988).

[23] K. H. Guber, H. Derrien, L. C. Leal, G. Arbanas, D. Wiarda, P. E. Koehler, and J. A. Harvey, "Astrophysical reaction rates for ^{58,60}Ni(n,γ) from new neutron capture cross section measurements," Phys. Rev. C 82, 057601 (2010).

[24] R. E. MacFarlane and A. C. Khaler, "Methods for Processing ENDF/B-VII with NJOY," Nuclear Data Sheets, 111, 2739-2890, 2010.

[25] R. O. Sayer, K. H. Guber, L. C. Leal, N. M. Larson, and T. Rauscher, "R-Matrix Evaluation of Cl Neutron Cross Sections up to 1.2 MeV," Oak Ridge National Laboratory, ORNL/TM-2003/50. See also R. O. Sayer, K. H. Guber, L. C. Leal, N. M. Larson, and T. Rauscher, "R-matrix Analysis of Cl Neutron Cross Sections up to 1.2-MeV," Phys. Rev. C73, 044603 (2006).

[26] R. O. Sayer and D. Wiarda, "RADCOP: Manipulation and Visualization of SAMMY Covariances,"C2117.pdf in Proc. of PHYSOR2006, American Nuclear Society Topical Meeting on Reactor Physics: Advances in Nuclear Analysis and Simulation, September 10 - 14, 2006, Vancouver, British Columbia, Canada.

[27] K. H. Guber, R. O. Sayer, T. E. Valentine, L. C. Leal, R. R. Spencer, J. A. Harvey, P. E. Koehler, and T. Rauscher, "New Maxwellian Average Neutron Capture Cross Sections for ^{35,37}Cl," Phys. Rev. C65, 058801 (2002).

[28] K. H. Guber, L. C. Leal, R. O. Sayer, P. E. Koehler, T. E. Valentine, H. Derrien, and J. A. Harvey, "Neutron Cross Section Measurements at ORELA for Improved Nuclear Data and their Application," Rad. Protection Dosimetry 116, 579 (2005); See also K. H. Guber, L. C. Leal, R. O. Sayer, P. E. Koehler, T. E. Valentine, H. Derrien, and J. A. Harvey, "New Neutron Cross-Section Measurements at ORELA and their Application in Nuclear Criticality Calculations," Nucl. Inst. Meth. Phys. Res. B241, 218 (2005);

[29] W. M. Good, J. A. Harvey, and N. W. Hill, "Neutron Total Cross Sections in the KeV Energy Range," Oak Ridge National Laboratory, ORNL-4937, p. 198 (1973); J. A. Harvey, private communication.

[30] S. Cierjacks, P. Forti, D. Kopsch, L. Kropp, J. Nebe, and H. Unseld, "High Resolution Total Neutron Cross Sections for Na, Cl, K, V, Mn and Co between 0.5 and 30 MeV," KFK-1000, (1969).

[31] U. N. Singh, H. I. Liou, G. Hacken, M. Slagowitz, F. Rahn, J. Rainwater, W. Makofske, and J. Garg, "Neutron Resonance Spectroscopy: Chlorine," Phys. Rev. C10, 2138 (1974).

[32] E. G. Joki, L. G. Miller, and J. E. Evans, "Total Neutron Cross Sections of Sodium, Potassium, and Rubidium in the 0.03 to 10 eV Region," Phillips Petroleum Report IDO-16276, 1955.

[33] D. C. Stupegia, M. Schmidt, C. R. Keedy, and A. A. Madson, "Neutron Capture Between 5 keV and 3 MeV," J. Nucl. Energ., 22, 267 (1968).

[34] J. B. Garg, R. L. Macklin, and L. Halperin, "Neutron Capture Cross Section of Manganese," Phys. Rev. C, 18, 2079, 1978.

[35] R. L. Macklin, "Resonance Neutron Capture by Manganese Below 2.5 keV," Nucl. Sci. Eng. 89, 362, 1985.

[36] L. Perrot, A. Billebaud, R. Brissot, A. Giorgni, D. Heuer,J.-M. Loiseaux, O. Meplan, and J.-B. Vianp, "Precise Validation of Database (n,γ) Cross Sections Using a Lead-Slowing-Down Spectrometer and Simulation from 0.1 eV to 30 eV: Methodology and Data for a Few Elements," Nuc. Sci. Eng. 144, 142-156, 2003.

[37] H. Derrien, L. C. Leal, N. M. Larson, K. Guber, D. Wiarda, and G. Arbanas, "Neutron resonance parameters of ^{55}Mn from Reich-Moore analysis of recent experimental neutron transmission and capture cross sections," International Conference on the Physics of Reactors "Nuclear Power: A Sustainable Resource" Casino-Kursaal Conference Center, Interlaken, Switzerland, September

14 - 19, 2008.

[38] J. A. Harvey, Private communication, Oak Ridge National Laboratory, Oak Ridge TN, USA, 2007.

[39] P. Shillebeeckx, Private communication, Institute for Reference Material And Measurements (IRMM), Geel, Belgium, 2007.

[40] K. H. Guber, P. E. Koehler, D. Wiarda, J. A. Harvey, T. E. Valentine, R. O. Sayer, L. C. Leal, N. M. Larson, T. S. Bigelow, C. Ausmus, D. R. Brashear, R. B. Overton, J. A. White, and V. M. Cauley, "New Neutron Cross Section Measurements from ORELA and New Resonance Evaluations," Proceedings of International Conference on Nuclear Data for Science and Technology, Nice, France, April 22 - 27, 2007.

[41] R. E. Cote, L. M. Bollinger, G. E. Thomas, "Total Neutron Cross Section of Manganese," Phys. Rev. 134, 5B, 1047, 1964.

[42] L. J. Rainwater, W. W. Havens, Jr., C. S. Wu, and J. R. Dunning, "Slow Neutron Velocity Spectrometer Studies I. Cd, Ag, Sb, Ir, Mn," Phys. Rev. 71, 65-79, 1947.

[43] F. Widder, "Neutron Capture Cross Section Measurements in the Energy Region from 0.01 to 10 Electron Volts," R-EIR-217, Institute For Reactor Physics, Wuerenlingen, Switzerland, April 1975.

[44] L. C. Leal, G. Arbanas, D. Wiarda, and H. Derrien, "Resonance Region Covariances Analysis Method and New Covariance Data for ^{232}Th, ^{233}U, ^{235}U, ^{238}U, and ^{239}Pu," Nuclear Data Sheets, Vol. 109, Issue 12, 28682873 (December 2008), Special Issue on Workshop on Neutron Cross Section Covariances, June 24 - 28, 2008, Port Jefferson, NY, USA.

[45] L. C. Leal, H. Derrien, J. A. Harvey, K. H. Guber, N. M. Larson, and R. R. Spencer, "R-Matrix Resonance Analysis and Statistical Properties of the Resonance Parameters of ^{233}U in the Neutron Energy Range from Thermal to 600 eV," Oak Ridge National Laboratory, ORNL/TM-2000/372 and ENDF-365 (2001).

[46] D. Wiarda, G. Arbanas, L. C. Leal, and M. E. Dunn, "Recent Advances with the AMPX Covariance Processing Capabilities in PUFF-IV," Nuclear Data Sheets, Vol. 109, Issue 12, 27912795 (December 2008), Special Issue on Workshop on Neutron Cross Section Covariances, June 24 - 28, 2008, Port Jefferson, NY, USA.

[47] L. C. Leal, H. Derrien, N. M. Larson, and R. Q. Wright, "R Matrix Analysis of ^{235}U Neutron Transmission and Cross Sections in the Energy Range 0 to 2.25 keV," Oak Ridge National Laboratory, ORNL/TM-13516 (1997).

[48] G. Arbanas, L. C. Leal, N. M. Larson, and H. Derrien, "Retroactive Covariance Matrix for ^{235}U in the Resolved-Resonance Region," Proc. of PHYSOR2006, American Nuclear Society Topical Meeting on Reactor Physics: Advances in Nuclear Analysis and Simulation, PHYSOR 2006, Vancouver, BC, Canada, September 10-14, 2006.

[49] P. Talou, T. Kawano, and P. G. Young, "Covariance Evaluation of ^{235}U, ^{238}U, and ^{239}Pu in the High Energy Range," in Proceedings of the 2007 Nuclear Data Conference, Nice, France.

[50] H. Derrien, L. C. Leal, N. M. Larson, and A. Courcelle, "Neutron Resonance Parameters of ^{238}U and Calculated Cross Sections from the Reich-Moore Analysis of Experimental Data in the Neutron Energy Range from 0 keV to 20 keV," Oak Ridge National Laboratory, ORNL/TM-2005/24 (2005).

[51] H. Derrien, L. C. Leal, and N. M. Larson, "Neutron Resonance Parameters and Covariance Matrix of ^{239}Pu," Oak Ridge National Laboratory, ORNL/TM-2008/123 (2008).

[52] Choong-Sup, L. Leal, Do Heon Kim, and Young-Ouk Lee, "A Sensitivity and uncertainty analysis of the k_{eff} values for fast and thermal benchmark with covariance data," International Conference on the Physics of Reactors, "Nuclear Power: A Sustainable Resource" Casino-Kursal Conference Center, Interlaken, Switzerland, September 14 - 19, 2008.

[53] International Handbook of Evaluated Criticality Safety Benchmark Experiments, NEA/NSC/DOC(95)03, OECD Nuclear Energy Agency (Rev., September 2007).

[54] Rearden, B.T., Hopper, C.M., Elam, K.R., Goluoglu, S., Parks, C.V. 2003. "Applications of the TSUNAMI Sensitivity and Uncertainty Analysis Methodology," pp. 6166 in Proceedings of the 7th International Conference on Nuclear Criticality Safety (ICNC2003), October 20 - 24, 2003, Tokai-Mura, Japan.

[55] S. Goluoglu, L. M. Petrie, Jr., M. Dunn, D. Hollenbach, and B. T. Rearden, "Monte Carlo Criticality Methods and Analysis Capabilities in SCALE," Nuclear Technology, Volume 174, Number 2, May 2011.

[56] SCALE: A Modular Code System for Performing Standardized Computer Analyses for Licensing Evaluations, NUREG/CR-0200, Rev. 7 (ORNL/NUREG/CSD-2/R7), Vols. I, II, and III (May 2004). Available from the Radiation Safety Information Computational Center at Oak Ridge National Laboratory as CCC-725.